

# On the analytical properties of the magneto-conductivity in the case of presence of stable open electron trajectories on a complex Fermi surface.

A.Ya. Maltsev.

*L.D. Landau Institute for Theoretical Physics  
142432 Chernogolovka, pr. Ak. Semenova 1A, maltsev@itp.ac.ru*

We consider the electric conductivity in normal metals in presence of a strong magnetic field. It is assumed here that the Fermi surface of a metal has rather complicated form such that different types of quasiclassical electron trajectories can appear on the Fermi level for different directions of  $\mathbf{B}$ . The effects we consider are connected with the existence of regular (stable) open electron trajectories which arise in general on complicated Fermi surfaces. The trajectories of this type have a nice geometric description and represent quasiperiodic lines with a fixed mean direction in the  $\mathbf{p}$ -space. Being stable geometric objects, the trajectories of this kind exist for some open regions in the space of directions of  $\mathbf{B}$ , which can be represented by “Stability Zones” on the unit sphere  $\mathbb{S}^2$ . The main goal of the paper is to give a description of the analytical behavior of conductivity in the Stability Zones, which demonstrates in general rather nontrivial properties.

## I. INTRODUCTION.

Our considerations here will be connected with the geometry of the quasiclassical electron trajectories on the Fermi surface in the presence of a strong magnetic field. The main goal of the paper is to give a detailed consideration of the contribution of the stable open trajectories to the conductivity tensor in the limit  $\omega_B \tau \rightarrow \infty$ . As we will see below, in spite of rather regular geometric properties of the stable (generic) open trajectories, their contribution to magneto-conductivity is quite non-trivial from analytical point of view, which is caused by nontrivial statistical properties of the trajectories of this kind. Here we will try to represent a general picture of the magneto-conductivity behavior in the case of presence of such trajectories on the Fermi surface, including the description of the dependence of conductivity on both the magnitude and the direction of  $\mathbf{B}$ . As we will see, both the structure of a “Stability Zone” on the angle diagram and the conductivity behavior in strong magnetic fields will demonstrate actually rather non-trivial properties.

We will base our considerations on the topological picture for the electron dynamics in the space of the quasimomenta, arising for general dispersion relation  $\epsilon(\mathbf{p})$  under the presence of a magnetic field. So, according to standard approach we will assume that the electron states in the conduction band are parametrized by the values of the quasimomenta  $\mathbf{p}$  which in fact should be considered as points of the three-dimensional space, factorized over the vectors of the reciprocal lattice:

$$\mathbb{T}^3 = \mathbb{R}^3 / \{n_1 \mathbf{a}_1 + n_2 \mathbf{a}_2 + n_3 \mathbf{a}_3\}, \quad n_1, n_2, n_3 \in \mathbb{Z}$$

The basis vectors of the reciprocal lattice are connected with the basis vectors  $(\mathbf{l}_1, \mathbf{l}_2, \mathbf{l}_3)$  of the direct lattice by the formulae

$$\mathbf{a}_1 = 2\pi\hbar \frac{\mathbf{l}_2 \times \mathbf{l}_3}{(\mathbf{l}_1, \mathbf{l}_2, \mathbf{l}_3)}, \quad \mathbf{a}_2 = 2\pi\hbar \frac{\mathbf{l}_3 \times \mathbf{l}_1}{(\mathbf{l}_1, \mathbf{l}_2, \mathbf{l}_3)},$$



FIG. 1: The canonical representation of the surfaces of genus 0, 1, 2 (etc ...).

$$\mathbf{a}_3 = 2\pi\hbar \frac{\mathbf{l}_1 \times \mathbf{l}_2}{(\mathbf{l}_1, \mathbf{l}_2, \mathbf{l}_3)}$$

and define the fundamental (Brillouen) zone in the  $\mathbf{p}$ -space.

The opposite faces of the parallelepiped formed by  $(\mathbf{a}_1, \mathbf{a}_2, \mathbf{a}_3)$  should be identified with each other, so the space of the electron states (for a given conduction band) represents in fact the three-dimensional torus  $\mathbb{T}^3$ . [38]

The dispersion relation  $\epsilon(\mathbf{p})$  can be considered either as a 3-periodic function in the  $\mathbf{p}$ -space or just as a smooth function on the compact manifold  $\mathbb{T}^3$ , given by the factorization of the  $\mathbf{p}$ -space over the reciprocal lattice  $L$ . In the same way, the constant energy levels  $\epsilon(\mathbf{p}) = \text{const}$  can be considered either as 3-periodic two-dimensional surfaces in the  $\mathbf{p}$ -space or as smooth compact surfaces  $S_\epsilon \subset \mathbb{T}^3$  embedded in the three-dimensional torus  $\mathbb{T}^3$ . Being considered in the last way, every nonsingular energy level represents a smooth compact orientable surface, which is topologically equivalent to one of the canonical surfaces defined by genus  $g$  (Fig. 1).

The genus  $g$  of the Fermi surface represents an important topological characteristic of the electron spectrum in metal. Another important topological characteristic of the electron spectrum is the way of embedding of the Fermi surface in  $\mathbb{T}^3$ . As an example, Fig. 2 represents an embedding of a genus 3 surface in the first Brillouen zone having “maximal rank”.

The quasiclassical evolution of the electron states in the presence of external homogeneous magnetic field  $\mathbf{B}$  can be described by the adiabatic equation (see e.g. [16,

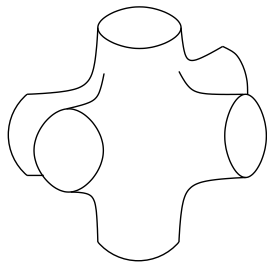


FIG. 2: The embedding of “maximal rank” of the surface of genus 3 in the torus  $\mathbb{T}^3$ .

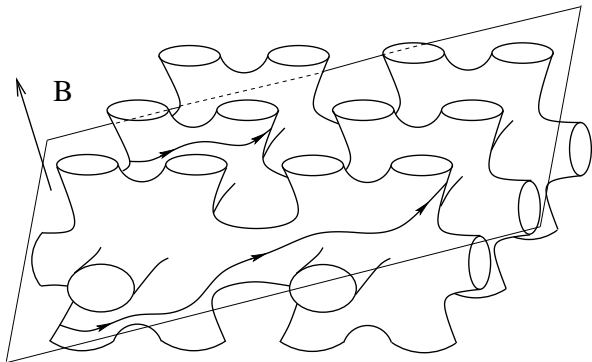


FIG. 3: The general picture of intersection of a complicated 3-periodic surface with the planes orthogonal to generic direction of  $\mathbf{B}$ .

35]):

$$\dot{\mathbf{p}} = \frac{e}{c} [\mathbf{v}_{\text{gr}}(\mathbf{p}) \times \mathbf{B}] = \frac{e}{c} [\nabla\epsilon(\mathbf{p}) \times \mathbf{B}] \quad (\text{I.1})$$

in the space of the quasimomenta.

The equation (I.1) is analytically integrable in  $\mathbf{p}$  - space and the quasiclassical trajectories are given by the intersections of the constant energy surfaces  $\epsilon(\mathbf{p}) = \text{const}$  with the planes orthogonal to  $\mathbf{B}$ . However, despite this analytical property of system (I.1), the global geometry of the quasiclassical trajectories in  $\mathbf{p}$  - space can be rather complicated. The reason for this circumstance is that the total  $\mathbf{p}$  - space is not compact while in  $\mathbb{T}^3$  the function  $\epsilon(\mathbf{p})$  represents the only one-valued integral of motion of (I.1). In general, we can expect rather complicated picture of intersection of the 3-periodic surface  $\epsilon(\mathbf{p}) = \text{const}$  with the planes orthogonal to general (totally irrational) direction of  $\mathbf{B}$  (see e.g. Fig. 3).

As it is usual for the case of normal metals, we will assume here that all the electron states with energies below the Fermi energy  $\epsilon_F$  are occupied by electrons, while all the electron states with energies above the Fermi energy are empty. The Fermi surface  $S_F : \epsilon(\mathbf{p}) = \epsilon_F$  represents a two-dimensional surface in  $\mathbb{T}^3$  separating occupied electron states from the empty ones. We have naturally  $\epsilon_{\min} < \epsilon_F < \epsilon_{\max}$  where  $\epsilon_{\min}$  and  $\epsilon_{\max}$  are

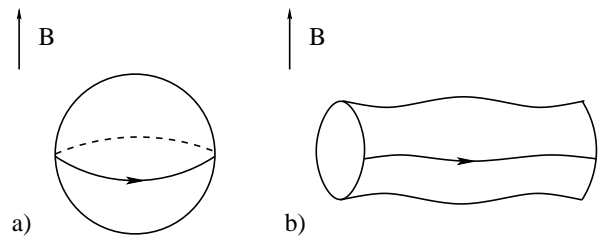


FIG. 4: Closed (a) and periodic (b) quasiclassical electron trajectories on different Fermi surfaces in  $\mathbf{p}$  - space (only one Brillouin zone is shown).

the minimal and maximal possible electron energies in the conductivity zone.

System (I.1) conserves the energy of a particle and also the phase volume element  $d^3p$ . As a consequence, the evolution according to system (I.1) does not change the Fermi distribution of the quasiparticles or more general temperature dependent equilibrium distributions

$$n(\mathbf{p}) = \frac{1}{e^{(\epsilon(\mathbf{p}) - \mu)/T} + 1}$$

However, it appears that the form of the trajectories of (I.1) plays an important role for the response of the electron system to the small electric fields  $\mathbf{E}$ , which defines the magneto-conductivity properties of normal metals. Due to the high degeneracy of the electron gas in metals, all the properties of such transport phenomena are defined in fact by the properties of system (I.1) just on the one energy level  $\epsilon = \epsilon_F$ , i.e. just on the one (Fermi) energy surface  $\epsilon(\mathbf{p}) = \epsilon_F$ .

The role of the global geometry of the quasiclassical electron trajectories in the transport phenomena in strong magnetic fields was first revealed by the school of I.M. Lifshitz (I.M. Lifshitz, M.Ya. Azbel, M.I. Kaganov, V.G. Peschansky) in 1950's (see [17–21, 23]). Thus, in paper [17] a crucial difference in contribution to magneto-conductivity of closed (Fig. 4, a) and open periodic (Fig. 4, b) quasiclassical trajectories in the limit  $B \rightarrow \infty$  was pointed out.

As was shown in [17], the contribution to the magneto-conductivity of the trajectories of the first kind is almost isotropic in the plane orthogonal to  $\mathbf{B}$  and has a rapidly decreasing character in this plane as  $B \rightarrow \infty$ . In contrast, the presence of the open periodic trajectories gives an additional contribution to the conductivity in the plane orthogonal to  $\mathbf{B}$ , which is strongly anisotropic in the limit  $B \rightarrow \infty$ . The asymptotic form of the conductivity tensor in the plane orthogonal to  $\mathbf{B}$  in the described cases can be represented as

$$\sigma^{\alpha\beta} \simeq \frac{ne^2\tau}{m^*} \begin{pmatrix} (\omega_B\tau)^{-2} & (\omega_B\tau)^{-1} \\ (\omega_B\tau)^{-1} & (\omega_B\tau)^{-2} \end{pmatrix}, \quad \omega_B\tau \rightarrow \infty \quad (\text{I.2})$$

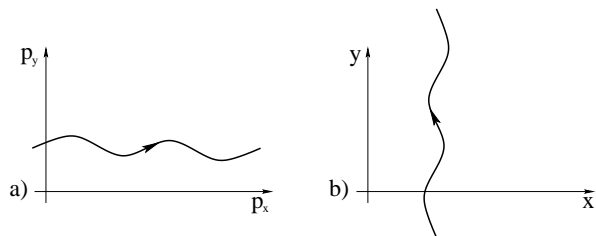


FIG. 5: The quasiclassical electron trajectory in  $\mathbf{p}$ -space (a) and its projection on the plane, orthogonal to  $\mathbf{B}$ , in  $\mathbf{x}$ -space (b).

(closed trajectories),

$$\sigma^{\alpha\beta} \simeq \frac{ne^2\tau}{m^*} \begin{pmatrix} (\omega_B\tau)^{-2} & (\omega_B\tau)^{-1} \\ (\omega_B\tau)^{-1} & * \end{pmatrix}, \quad \omega_B\tau \rightarrow \infty \quad (\text{I.3})$$

(open periodic trajectories), after an appropriate choice of coordinates. (Here and below the notation  $*$  means just a constant of the order of unity).

The formulae (I.2) - (I.3) represent the asymptotic form of the conductivity tensor, so all the equalities give actually just the order of the absolute value of the corresponding quantities.

The value  $m^*$  represents here just some (approximate) effective mass of electron in crystal and  $\tau$  denotes the mean free electron time defined by the intensity of the scattering processes.

The value

$$\omega_B \simeq \frac{eB}{m^*c}$$

can be considered as an “approximate value” of the cyclotron frequency in the crystal. From geometrical point of view  $\omega_B$  represents approximately the inverse time of motion along a closed trajectory (Fig. 4, a) or the inverse time of motion through one Brillouin zone for periodic open trajectories (Fig. 4, b). It becomes clear from this point of view that the global geometry of the quasiclassical trajectories reveals exactly in the limit  $\omega_B\tau \rightarrow \infty$  when the mean free electron time exceeds the time of motion inside one Brillouin zone. Let us say here that for experimental observation of the “geometric strong magnetic field limit” rather pure materials under rather low temperatures ( $T \sim 1K$ ) and rather strong magnetic fields ( $B \sim 10^4 Gs$ ) should be usually used.

In formula (I.3) the  $x$ -axis is chosen along the mean direction of the periodic trajectories in  $\mathbf{p}$ -space. As can be easily derived from system (I.1), the projection of the corresponding trajectory in coordinate space onto the plane orthogonal to  $\mathbf{B}$  is given just by the rotation of the trajectory in  $\mathbf{p}$ -space by  $90^\circ$  (Fig. 5).

We can see then that even very strong magnetic field does not block the electron motion along the  $y$ -axis in the coordinate space in the presence of the trajectories shown at Fig. 4, b. As a result, the  $y$ -component of

conductivity in the plane orthogonal to  $\mathbf{B}$  remains finite in the limit  $\omega_B\tau \rightarrow \infty$ . The strong anisotropy of the conductivity tensor in this situation gives an experimental possibility to observe this phenomenon as well as to determine the mean direction of the open trajectories in  $\mathbf{p}$ -space.

The conductivity along the direction of  $\mathbf{B}$  remains finite in the limit  $\omega_B\tau \rightarrow \infty$  in both the cases described above. The asymptotic forms of the full conductivity tensor in  $\mathbf{x}$ -space can be represented as:

$$\sigma^{kl} \simeq \frac{ne^2\tau}{m^*} \begin{pmatrix} (\omega_B\tau)^{-2} & (\omega_B\tau)^{-1} & (\omega_B\tau)^{-1} \\ (\omega_B\tau)^{-1} & (\omega_B\tau)^{-2} & (\omega_B\tau)^{-1} \\ (\omega_B\tau)^{-1} & (\omega_B\tau)^{-1} & * \end{pmatrix}, \quad \omega_B\tau \rightarrow \infty \quad (\text{I.4})$$

(closed trajectories),

$$\sigma^{kl} \simeq \frac{ne^2\tau}{m^*} \begin{pmatrix} (\omega_B\tau)^{-2} & (\omega_B\tau)^{-1} & (\omega_B\tau)^{-1} \\ (\omega_B\tau)^{-1} & * & * \\ (\omega_B\tau)^{-1} & * & * \end{pmatrix}, \quad \omega_B\tau \rightarrow \infty \quad (\text{I.5})$$

(open periodic trajectories).

Let us note here that both the trajectories shown at Fig. 4 are actually closed in the torus  $\mathbb{T}^3$ . However, their embeddings in  $\mathbb{T}^3$  are completely different from topological point of view. Thus, the embedding of the trajectory shown at Fig. 4, a is “homologous” to zero, while the embedding of the trajectory shown at Fig. 4, b represents a nonzero homology class in  $\mathbb{T}^3$ . Certainly, the difference between the trajectories shown at Fig. 4, a and Fig. 4, b is more evident in the covering  $\mathbf{p}$ -space where they have different global geometry.

Let us say here also, that both the situations shown at Fig. 4 a,b represent the special case when the conductivity tensor can be represented as a regular series in powers of  $(\omega_B\tau)^{-1}$  in the limit  $\omega_B\tau \rightarrow \infty$ . Thus, we can actually write here

$$\begin{aligned} \sigma^{kl}(B) &\simeq \frac{ne^2\tau}{m^*} \begin{pmatrix} 0 & 0 & 0 \\ 0 & 0 & 0 \\ 0 & 0 & * \end{pmatrix} + \\ &+ \frac{ne^2\tau}{m^*} \begin{pmatrix} 0 & * & * \\ * & 0 & * \\ * & * & 0 \end{pmatrix} (\omega_B\tau)^{-1} + \\ &+ \frac{ne^2\tau}{m^*} \begin{pmatrix} * & * & * \\ * & * & * \\ * & * & * \end{pmatrix} (\omega_B\tau)^{-2} + \dots \quad (\text{I.6}) \end{aligned}$$

(closed trajectories),

$$\begin{aligned} \sigma^{kl}(B) &\simeq \frac{ne^2\tau}{m^*} \begin{pmatrix} 0 & 0 & 0 \\ 0 & * & * \\ 0 & * & * \end{pmatrix} + \\ &+ \frac{ne^2\tau}{m^*} \begin{pmatrix} 0 & * & * \\ * & 0 & * \\ * & * & 0 \end{pmatrix} (\omega_B\tau)^{-1} + \\ &+ \frac{ne^2\tau}{m^*} \begin{pmatrix} * & * & * \\ * & * & * \\ * & * & * \end{pmatrix} (\omega_B\tau)^{-2} + \dots \quad (\text{I.7}) \end{aligned}$$

(open periodic trajectories), where the even powers of  $\omega_B\tau$  correspond to the symmetric part of  $\sigma^{kl}(B)$ , while the odd powers of  $\omega_B\tau$  represent the anti-symmetric part in accordance with the Onsager relations.

As we will see below, this situation does not take place for general open electron trajectories on the Fermi surface.

In papers [18, 19] different examples of complicated Fermi surfaces and more general types of open electron trajectories in strong magnetic fields were considered. The trajectories considered in [18, 19] are in general not periodic and are non-closed both in  $\mathbb{T}^3$  and the  $\mathbf{p}$ -space and represent the first examples of the stable open electron trajectories on a complicated Fermi surface. The form of the trajectories found in [18, 19] demonstrates also strongly anisotropic properties, so the strong anisotropy of the conductivity tensor in the limit  $\omega_B\tau \rightarrow \infty$  is also expected in this case. As was pointed out in [15], the analytical behavior of conductivity in these examples can in fact be different from (I.5) and demonstrate a slower approach to its limiting form in the interval of not extremely strong magnetic fields. Here we will try to study this question in general case using the topological description of the stable open trajectories on the Fermi surface.

In the survey articles [20–22] and also in the book [23] a remarkable review of both the theoretical and experimental investigations of this branch of electron theory of metals made at that time can be found. Let us give here also a reference on a survey article [15] where the same topics were revisited after forty years and which contains also the aspects appeared in the later period.

The general problem of classification of all possible types of trajectories of dynamical system (I.1) with arbitrary (periodic) dispersion law  $\epsilon(\mathbf{p})$  was set by S.P. Novikov ([27]) and was intensively investigated in his topological school (S.P. Novikov, A.V. Zorich, S.P. Tsarev, I.A. Dynnikov). The topological investigation of system (I.1) has led to rather detailed understanding of the geometry of the trajectories of different types and gave finally the full classification of all possible types of trajectories of (I.1). One of the most important parts of the mathematical theory of the trajectories of (I.1), which will be also of great importance in the present paper, is connected with the detailed description of the

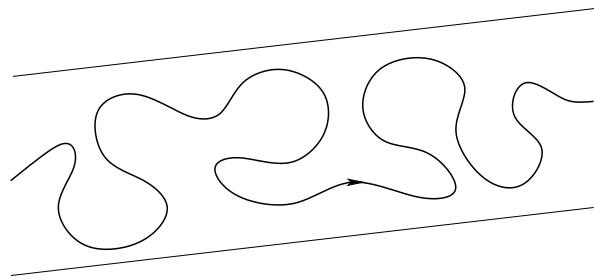


FIG. 6: A stable (quasiperiodic) open trajectory of system (I.1) passing through a straight strip of a finite width in the plane orthogonal to  $\mathbf{B}$ .

stable open trajectories of system (I.1). Let us say here that the most important breakthroughs in this problem were made in papers [8, 36] where rather deep topological theorems about non-closed trajectories of system (I.1) were proved.

Using the topological description of the stable open trajectories of system (I.1) it was possible to introduce important topological characteristics of the stable non-trivial regimes of the magneto-conductivity behavior in the limit  $\omega_B\tau \rightarrow \infty$ , which were introduced in paper [28]. In general, the characteristics introduced in [28] can be described in the following way:

Let us exclude now the “trivial” cases when we have just closed electron trajectories on the Fermi surface in  $\mathbf{p}$ -space and consider the situation when open trajectories (in  $\mathbf{p}$ -space) are present on the Fermi level. Besides that, let us require that the open trajectories are stable with respect to small rotations of  $\mathbf{B}$  such that we have a “Stability Zone” in the space of directions of  $\mathbf{B}$ , where similar open trajectories exist on the Fermi level.

As can be extracted from the topological description of the stable open trajectories of system (I.1), the trajectories of this type demonstrate the following remarkable properties:

- 1) Every stable open (in  $\mathbf{p}$ -space) trajectory of (I.1) lies in a straight strip of a finite width in the plane orthogonal to  $\mathbf{B}$ , passing through it from  $-\infty$  to  $+\infty$  (Fig. 6);
- 2) The mean direction of all open stable trajectories in  $\mathbf{p}$ -space is given by the intersection of the plane orthogonal to  $\mathbf{B}$  and some integral (generated by two reciprocal lattice vectors) plane  $\Gamma$ , which is the same for a given “Stability Zone” in the space of directions of  $\mathbf{B}$ .

Let us note here that the statement (1) was first formulated by S.P. Novikov in the form of a conjecture, which was proved later for the stable open trajectories of (I.1) ([8, 36]).

As was pointed out in [28], the integral planes  $\Gamma_\alpha$  represent experimentally observable objects view the remarkable geometric properties of the open stable trajectories, described above. Thus, measuring the conductivity in the limit  $\omega_B\tau \rightarrow \infty$ , we can observe strongly

anisotropic behavior of conductivity in the planes orthogonal to  $\mathbf{B}$  for all  $\mathbf{B}/B \in \Omega_\alpha$  and extract the integral plane  $\Gamma_\alpha$ , which is swept by the directions of the highest decreasing of conductivity in the  $\mathbf{x}$  - space.

More precisely, let us introduce the values

$$\sigma_\infty^{kl}(\mathbf{B}/B) = \lim_{\omega_B\tau \rightarrow \infty} \sigma^{kl}(\mathbf{B}) \quad , \quad k, l = 1, 2, 3$$

Then, we can chose a basis in  $\mathbf{x}$  - space

$$\left( \mathbf{e}_1(\mathbf{B}), \mathbf{e}_2(\mathbf{B}), \mathbf{e}_3 = \mathbf{B}/B \right) \quad ,$$

smoothly depending on  $\mathbf{B}$  in  $\Omega_\alpha$ , where the values  $\sigma_\infty^{kl}$  will have the form

$$\sigma_\infty^{kl} = \frac{ne^2\tau}{m^*} \begin{pmatrix} 0 & 0 & 0 \\ 0 & * & * \\ 0 & * & * \end{pmatrix} \quad (\text{I.8})$$

As was said above, the direction of the vector  $\mathbf{e}_1(\mathbf{B})$  is given by the intersection of the plane orthogonal to  $\mathbf{B}$  with an integral plane, i.e. the plane generated by two reciprocal lattice vectors  $\mathbf{q}_1, \mathbf{q}_2$ , which is the same for the Zone  $\Omega_\alpha$ .

The integral plane  $\Gamma_\alpha$  can be represented by an indivisible triple of integer numbers  $(M_\alpha^1, M_\alpha^2, M_\alpha^3)$  according to the equation

$$M_\alpha^1(\mathbf{x}, \mathbf{l}_1) + M_\alpha^2(\mathbf{x}, \mathbf{l}_2) + M_\alpha^3(\mathbf{x}, \mathbf{l}_3) = 0 \quad (\text{I.9})$$

where  $(\mathbf{l}_1, \mathbf{l}_2, \mathbf{l}_3)$  are the basis direct lattice vectors. The numbers  $(M_\alpha^1, M_\alpha^2, M_\alpha^3)$  were called in [28] the topological quantum numbers observable in conductivity of normal metals. Let us say here that the triples  $(M_\alpha^1, M_\alpha^2, M_\alpha^3)$  can be rather nontrivial for complicated Fermi surfaces.

The complete Zone  $\Omega_\alpha$  can be called here the mathematical Stability Zone, corresponding to a given Fermi energy. We have to say here, however, that in experimental study of magneto-conductivity it is natural to introduce extended “experimentally observable Stability Zone”  $\hat{\Omega}_\alpha$  ( $\Omega_\alpha \subset \hat{\Omega}_\alpha$ ) due to specific behavior of trajectories of system (I.1) near the boundary of  $\Omega_\alpha$ . Everywhere in  $\hat{\Omega}_\alpha$  the behavior of conductivity is experimentally indistinguishable from that in  $\Omega_\alpha$  even under good formal implementation of the condition  $\omega_B\tau \gg 1$  until the magnitude  $B$  of magnetic field becomes extremely high. The conventional form of  $\hat{\Omega}_\alpha$  depends actually on the experimental conditions and is determined mainly by the maximal values of  $B$  in experiment. The difference between the Zones  $\hat{\Omega}_\alpha$  and  $\Omega_\alpha$ , which can be detected only in extremely strong magnetic fields, represents in fact one of essential features of analytical behavior of conductivity, considered here.

Let us note now that the stable open quasiclassical trajectories do not represent all possible types of non-closed trajectories of system (I.1) and trajectories with more complicated geometry can arise on complicated Fermi

surfaces for some special directions of  $\mathbf{B}$ . Thus, the first example of trajectory which can not be restricted by any straight strip of a finite width was constructed by S.P. Tsarev ([34]). The trajectory of Tsarev demonstrates explicit chaotic behavior on the Fermi surface and is essentially different from the stable open trajectories from this point of view. On the other hand, the Tsarev trajectory is also strongly anisotropic in the  $\mathbf{p}$  - space and has an asymptotic direction in the plane orthogonal to  $\mathbf{B}$ . So, from experimental point of view the contribution of Tsarev trajectories to the magneto-conductivity is also strongly anisotropic in the limit  $\omega_B\tau \rightarrow \infty$  and corresponds to the regime (I.8). Let us say, however, that the Tsarev chaotic trajectories are completely unstable under small rotations of  $\mathbf{B}$  and are not connected with topologically stable characteristics unlike the stable open trajectories discussed above. We have to say also, that the trajectories of Tsarev type (if they present) can appear just for the set of zero measure in the space of directions of  $\mathbf{B}$ .

Another example of non-closed trajectory of (I.1) which demonstrates strongly chaotic behavior both in  $\mathbb{T}^3$  and in  $\mathbf{p}$  - space was constructed by I.A. Dynnikov in [9]. The trajectories of Dynnikov are rather different from the Tsarev chaotic trajectories and require the maximal irrationality of the direction of  $\mathbf{B}$  to be observed. The behavior of the conductivity tensor in the presence of the chaotic trajectories constructed in [9] was investigated in [24] and appeared to be rather different from both the regimes given by (I.4) and (I.5). The most interesting feature of the contribution to the conductivity tensor of the trajectories of this kind is that the presence of such trajectories suppresses the conductivity in all directions, including the direction of  $\mathbf{B}$ , in the limit  $\omega_B\tau \rightarrow \infty$ .

In general, the Tsarev and Dynnikov chaotic trajectories demonstrate two different general types of possible chaotic behavior of trajectories of system (I.1), so in this sense all chaotic trajectories of (I.1) can be attributed to the Tsarev or Dynnikov type. Let us say here that different properties of chaotic trajectories of system (I.1) are also intensively investigated in modern mathematical literature (see [3–7, 10–12, 32, 33, 37]).

The directions of  $\mathbf{B}$ , corresponding to the chaotic open trajectories, can appear only outside the “Stability Zones”, corresponding to the stable open trajectories of system (I.1). In the same way, the chaotic open trajectories of different types (Tsarev or Dynnikov type) can not appear at the same direction of  $\mathbf{B}$ . Let us say, however, that in general the contribution of non-closed trajectories to the conductivity tensor should be added with the contribution (I.4) of closed trajectories of system (I.1), which usually present together with open trajectories (of any kind) at the same Fermi surface.

For more rigorous description of possible situations in the behavior of trajectories of (I.1) with arbitrary periodic dispersion law let us give here a reference to a detailed mathematical survey [10], devoted to this question. The detailed consideration of different physical re-

sults based on the results of topological investigations of system (I.1) can be found in [25, 26, 29].

Our main goal in this paper will be more detailed investigation of the conductivity behavior in the “Stability Zones”, based on the detailed topological description of the stable open electron trajectories arising for the corresponding directions of  $\mathbf{B}$ . As we said already, the corresponding stable open trajectories demonstrate rather regular geometric properties in the planes orthogonal to  $\mathbf{B}$ . Thus, all the stable open trajectories have the form shown at Fig. 6 and the same mean direction in  $\mathbf{p}$ -space, given by the intersection of the plane orthogonal to  $\mathbf{B}$  with an integral plane  $\Gamma_\alpha$ , which is fixed for the corresponding Stability Zone  $\Omega_\alpha$ . As a result, the conductivity tensor has the asymptotic form (I.8) in the limit  $\omega_B\tau \rightarrow \infty$  and demonstrates the specific geometric properties described above. These geometric (or topological) properties of the conductivity tensor give the most stable (topological) characteristics of the conductivity for a given “Stability Zone” and are connected with the “purely geometric” limit  $\omega_B\tau \rightarrow \infty$ . At the same time, we will see below, that the conductivity tensor demonstrates in general rather nontrivial analytical dependence on  $\mathbf{B}$  in different parts of “experimentally observable” Stability Zones, which is caused by specific features of different trajectories of system (I.1) in these regions. Here we will investigate the analytical properties of conductivity for the case of rather big (but finite) values of the parameter  $\omega_B\tau$  using topological description of “carriers of open trajectories” on the Fermi surface, defined for the corresponding directions of  $\mathbf{B}$ . As we will see below, both the dependence on the parameter  $\omega_B\tau$  and on the direction of  $\mathbf{B}$  demonstrate here rather nontrivial properties.

In the next section we will give a description of “experimentally observable” Stability Zone and try to describe the main features of the analytical behavior of conductivity in its different parts, which gives from our point of view the main points of the picture arising in general case. In Sections III and IV we will present more detailed consideration of the contribution of the stable open trajectories to the magneto-conductivity, based on the topological description of such trajectories on complicated Fermi surfaces. Sections III and IV will have more mathematical character in comparison with Section II.

## II. THE ANALYTICAL BEHAVIOR OF CONDUCTIVITY IN THE EXPERIMENTALLY OBSERVABLE STABILITY ZONE.

To describe briefly the general picture, let us point out now the main points, which will play the most essential role in our considerations below. This section will be mostly descriptive, while more detailed analysis will be presented in Sections III, IV.

As we said already, the stable open trajectories demonstrate quasiperiodic properties for generic directions of  $\mathbf{B}$  ( $\mathbf{B}/B \in \Omega_\alpha$ ). However, they become purely periodic for some special directions of the magnetic field. It’s not difficult to see that the last situation arises every time when the plane orthogonal to  $\mathbf{B}$  intersects the plane  $\Gamma_\alpha$  along an integer vector in  $\mathbf{p}$ -space:

$$\mathbf{a} = k_1 \mathbf{q}_1 + k_2 \mathbf{q}_2 = m_1 \mathbf{a}_1 + m_2 \mathbf{a}_2 + m_3 \mathbf{a}_3 \quad (\text{II.1})$$

( $k_1, k_2, m_1, m_2, m_3 \in \mathbb{Z}$ ).

Both the cases of the quasiperiodic and the periodic trajectories lead in this situation to the conductivity tensor (I.8) in the limit  $\omega_B\tau \rightarrow \infty$ , having the same stable geometric properties for a given “Stability Zone”. However, as we will see below, the limiting values of the components  $\sigma^{22}, \sigma^{23}, \sigma^{32}, \sigma^{33}$ , i.e. the values

$$\sigma_\infty^{kl}(\mathbf{B}/B) = \lim_{\omega_B\tau \rightarrow \infty} \sigma^{kl}(\mathbf{B}) \quad , \quad k, l = 2, 3$$

( $\mathbf{B}/B$  is fixed), will have here sharp “jumps” with respect to the same values, defined for close generic directions of  $\mathbf{B}$ .

More precisely, we can introduce the functions  $\bar{\sigma}_\infty^{kl}(\mathbf{B}/B)$ , ( $k, l = 2, 3$ ), which represent continuous functions of  $\mathbf{n} = \mathbf{B}/B$  in  $\Omega_\alpha$  and coincide with the corresponding values  $\sigma_\infty^{kl}(\mathbf{B}/B)$  for generic directions  $\mathbf{B}/B \in \Omega_\alpha$ . However, for special directions of  $\mathbf{B}$  described above we will have  $\sigma_\infty^{kl}(\mathbf{B}/B) \neq \bar{\sigma}_\infty^{kl}(\mathbf{B}/B)$ , which is caused by special features of statistical averaging over the open trajectories of (I.1) near the Fermi surface. It’s not difficult to show also that we will always have the inequalities

$$\sigma_\infty^{22}(\mathbf{B}/B) - \bar{\sigma}_\infty^{22}(\mathbf{B}/B) > 0 \quad ,$$

$$\sigma_\infty^{33}(\mathbf{B}/B) - \bar{\sigma}_\infty^{33}(\mathbf{B}/B) > 0$$

for these special directions of  $\mathbf{B}$ , while the signs of  $\sigma_\infty^{kl}(\mathbf{B}/B) - \bar{\sigma}_\infty^{kl}(\mathbf{B}/B)$ ,  $k \neq l$ , are in general indefinite.

The directions  $\mathbf{B}/B \in \Omega_\alpha$ , corresponding to a fixed rational mean direction  $\mathbf{a}$  of open trajectories, represent a one-dimensional curve  $\gamma_{\mathbf{a}}^\alpha$  (on  $\mathbb{S}^2$ ) given by the intersection of the big circle, orthogonal to  $\mathbf{a}$ , and the Stability Zone  $\Omega_\alpha$  (Fig. 7 a). We have to say, however, that according to a more detailed consideration the periodic trajectories exist actually on some bigger curve  $\hat{\gamma}_{\mathbf{a}}^\alpha$  representing extension of the curve  $\gamma_{\mathbf{a}}^\alpha$  outside the Stability Zone  $\Omega_\alpha$  (Fig. 7 b). All the open trajectories have the same mean direction  $\mathbf{a}$  for all  $\mathbf{B}/B \in \hat{\gamma}_{\mathbf{a}}^\alpha$  and the area covered by the periodic trajectories on the Fermi surface vanishes at the endpoints of  $\hat{\gamma}_{\mathbf{a}}^\alpha$ . The open periodic trajectories demonstrate stability properties inside the Stability Zone  $\Omega_\alpha$  and become unstable outside  $\Omega_\alpha$  on the curve  $\hat{\gamma}_{\mathbf{a}}^\alpha$ . Let us note also here that the measure of generic (quasiperiodic) open trajectories on the Fermi surface remains finite up to the boundary of

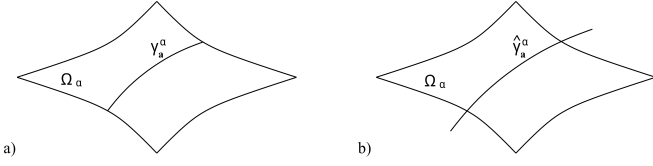


FIG. 7: (a) A schematic representation of the family  $\gamma_{\mathbf{a}}^\alpha$  of special directions of  $\mathbf{B}$ , corresponding to a rational mean direction  $\mathbf{a}$  of open trajectories, within a Stability Zone  $\Omega_\alpha$ . (b) The full one-dimensional set  $\hat{\gamma}_{\mathbf{a}}^\alpha$  of directions of  $\mathbf{B}$ , corresponding to existence of periodic trajectories with mean direction  $\mathbf{a}$ , intersecting the Stability Zone  $\Omega_\alpha$ .

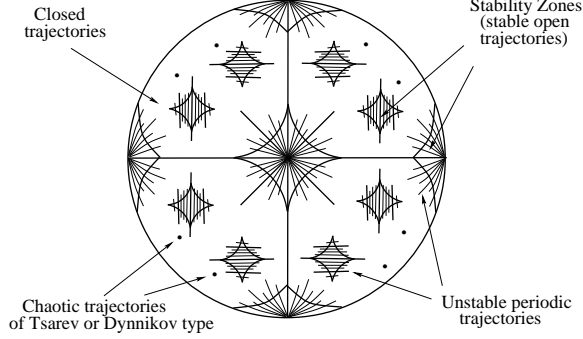


FIG. 8: A schematic angle diagram showing different situations for different directions of  $\mathbf{B}$  on the unit sphere.

a Stability Zone. In general, the schematic angle diagram corresponding to a complicated Fermi surface can be represented by Fig. 8.[39]

We can see then that every Stability Zone  $\Omega_\alpha$  is actually covered by an everywhere dense net representing the “special directions” of  $\mathbf{B}$  corresponding to different rational mean directions  $\mathbf{a}$  of the stable open trajectories (Fig. 9). The set of all possible rational mean directions  $\mathbf{a}$  of the open trajectories is given by two conditions:

- 1)  $\mathbf{a} \in \Gamma_\alpha$ ,
- 2)  $C_{\mathbf{a}} \cap \Omega_\alpha \neq \emptyset$ ,

where  $C_{\mathbf{a}}$  is the big circle orthogonal to the direction  $\mathbf{a}$ . Everywhere on the net we have the situation

$$\sigma_\infty^{kl}(\mathbf{B}/B) \neq \bar{\sigma}_\infty^{kl}(\mathbf{B}/B) ,$$

however, the difference

$$|\sigma_\infty^{kl}(\mathbf{B}/B) - \bar{\sigma}_\infty^{kl}(\mathbf{B}/B)|$$

decreases with the growth of the numbers  $(m_1, m_2, m_3)$  in (II.1). As we will see below, the approximate evaluation for this difference for complicated Fermi surfaces can be written in the form

$$|\sigma_\infty^{kl}(\mathbf{B}/B) - \bar{\sigma}_\infty^{kl}(\mathbf{B}/B)| \sim \frac{\ln^2(|m_1| + |m_2| + |m_3|)}{(|m_1| + |m_2| + |m_3|)^2} , \quad (\text{II.2})$$

$(k, l = 2, 3).$

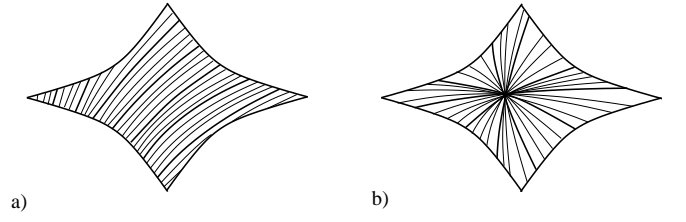


FIG. 9: The dense nets of directions of  $\mathbf{B}$  inside  $\Omega_\alpha$ , corresponding to arising of periodic trajectories, in the cases when the direction orthogonal to  $\Gamma_\alpha$  does not belong to  $\Omega_\alpha$  (a) and when this direction belongs to  $\Omega_\alpha$  (b).

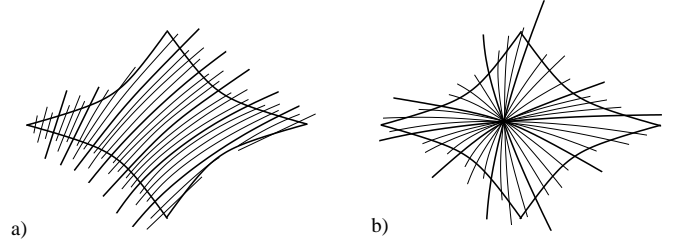


FIG. 10: The full sets of directions of  $\mathbf{B}$  near  $\Omega_\alpha$ , corresponding to arising of periodic trajectories on the Fermi surface.

In the physical situation, when the values of  $\mathbf{B}$  are finite but rather big, the “jumps” on the curves  $\gamma_{\mathbf{a}}^\alpha$  become very sharp “peaks” on these curves, which can be called the “rational peaks” in the values of magnetoconductivity according to rationality of the mean direction of the corresponding open trajectories in  $\mathbf{p}$ -space.

The second important point in our picture is connected with the behavior of trajectories of system (I.1) near the boundaries of the Stability Zones  $\Omega_\alpha$  outside the Stability Zones. As we have already said, the periodic trajectories of system (I.1) on the Fermi level exist in fact for directions of  $\mathbf{B}$  belonging to the extended curves  $\hat{\gamma}_{\mathbf{a}}^\alpha$ , so only at the endpoints of  $\hat{\gamma}_{\mathbf{a}}^\alpha$  the measure of the trajectories with the period  $\mathbf{a}$  on the Fermi surface is equal to zero. As a result, the full set of directions of  $\mathbf{B}$  near  $\Omega_\alpha$ , corresponding to the presence of open trajectories on the Fermi level, represents the Stability Zone  $\Omega_\alpha$  with a set of additional segments near  $\Omega_\alpha$ , which is dense on the boundary of  $\Omega_\alpha$  (Fig. 10). [40]

At the same time, the measure of open trajectories on the Fermi surface for generic directions  $\mathbf{B}/B \notin \hat{\gamma}_{\mathbf{a}}^\alpha$  remains finite up to the boundary of the Stability Zone and jumps abruptly to zero outside  $\Omega_\alpha$ . The transformation of the open trajectories on the boundary of  $\Omega_\alpha$  leads in this case to appearance of very long closed trajectories near the boundary of  $\Omega_\alpha$  which are very similar to open trajectories from experimental point of view up to very (extremely) high values of  $B$ . We can state then that in experimental observation of conductivity we observe actually some “extended Stability Zone”  $\Omega_\alpha$ , including the

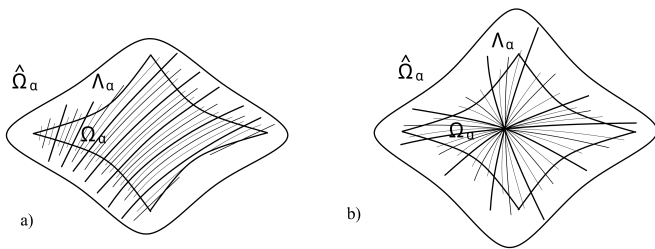


FIG. 11: The “extended Zones”  $\hat{\Omega}_\alpha$  observable in experiments.

exact Stability Zone as a subset. The boundaries of the “extended Zone”  $\hat{\Omega}_\alpha$  are in a sense conditional and depend on the maximal values of  $B$  used in the experiment. We can claim, however, that the experimentally observable Stability Zone exceeds the exact Stability Zone by a set of a finite measure for any arbitrary big maximal value of magnetic field  $B_{max}$  (see Fig. 11).

The set  $\Lambda_\alpha = \hat{\Omega}_\alpha / \Omega_\alpha$  can be called a “supplement” to the Stability Zone  $\Omega_\alpha$  arising in the experimental observation of conductivity in strong magnetic fields.

It is possible to introduce also the values  $\sigma_\infty^{kl}(\mathbf{B}/B)$  and  $\bar{\sigma}_\infty^{kl}(\mathbf{B}/B)$ , in the regions  $\Lambda_\alpha$ , which will have the same meaning as in the regions  $\Omega_\alpha$ . In these regions we will have identically:  $\bar{\sigma}_\infty^{22} \equiv \bar{\sigma}_\infty^{23} \equiv \bar{\sigma}_\infty^{32} \equiv 0$ . Like in  $\Omega_\alpha$ , we will have here  $\sigma_\infty^{kl}(\mathbf{B}/B) \equiv \bar{\sigma}_\infty^{kl}(\mathbf{B}/B)$  for generic directions of  $\mathbf{B}$  and in general  $\sigma_\infty^{kl}(\mathbf{B}/B) \neq \bar{\sigma}_\infty^{kl}(\mathbf{B}/B)$  for  $\mathbf{B}/B \in \hat{\gamma}_\mathbf{a}^\alpha$ .

Both inside the regions  $\Omega_\alpha$  and  $\Lambda_\alpha$  the approach of the values of  $\sigma^{kl}$  to their limiting values  $\sigma_\infty^{kl}$  is rather irregular (but with some general trend), which makes the conductivity behavior rather nontrivial from the experimental point of view even for the values of  $B$ , satisfying the formal criterion  $\omega_B \tau \gg 1$ .

First, as we have already noted, the values  $\sigma_\infty^{kl}(\mathbf{B}/B)$  are different from the values  $\bar{\sigma}_\infty^{kl}(\mathbf{B}/B)$  on the curves  $\hat{\gamma}_\mathbf{a}^\alpha$  both in the regions  $\Omega_\alpha$  and  $\Lambda_\alpha$ . These values are continuous along every curve  $\hat{\gamma}_\mathbf{a}^\alpha$  up to the boundary of the Zone  $\hat{\Omega}_\alpha$  (more precisely, up to the endpoints of  $\hat{\gamma}_\mathbf{a}^\alpha$ ), at the same time, they are discontinuous in the transverse directions to  $\hat{\gamma}_\mathbf{a}^\alpha$ .

Formally speaking, all the open trajectories in the Zone  $\Lambda_\alpha$  are periodic, so their contribution to magneto-conductivity can be represented in the regular form (I.5). However, as can be easily seen, the period of the trajectories given by formula (II.1) can be rather large for big numbers  $(m_1, m_2, m_3)$ . As a result, the features of the regular expansion can be observed actually just on the scales

$$\omega_B \tau \gg |m_1| + |m_2| + |m_3| .$$

At the same time, on the scales of the values of  $B$ , satisfying the condition

$$1 < \omega_B \tau < |m_1| + |m_2| + |m_3| , \quad (\text{II.3})$$

the contribution of the periodic trajectories reveals the properties, analogous to those corresponding to generic open trajectories. We can state then, that for big values of  $|m_1| + |m_2| + |m_3|$  the periodic open trajectories are indistinguishable from the generic ones if the values of  $B$  satisfy restriction (II.3). Let us say here also, that under the same restrictions on  $B$  the periodic open trajectories are also indistinguishable from the long closed trajectories in the vicinity of the curve  $\hat{\gamma}_\mathbf{a}^\alpha$  in the Zone  $\Lambda_\alpha$ .

Let us now make some remarks concerning the experimental study of the magneto-conductivity in (monocrystalline) metals having complicated Fermi surfaces. Let us note first that the measuring the magneto-conductivity in presence of the open trajectories very often is being made for directions of  $\mathbf{B}$  belonging to the largest “Stability Zones”, characterized by the biggest area and the highest symmetry on the angle diagram. Rather often it is convenient also to fix just a small set of directions of  $\mathbf{B}$  inside the Stability Zone and to measure the magneto-conductivity changing the magnitude  $B$  of the magnetic field. According to the design of the research facility it appears rather often that the corresponding set of directions of  $\mathbf{B}$  represents in fact some symmetric or “rational” points on the angle diagram, such that all (or a part) the directions belong actually to some curves  $\hat{\gamma}_\mathbf{a}^\alpha \subset \hat{\Omega}_\alpha$  corresponding to rather simple periods  $\mathbf{a}$  of the open trajectories. This is exactly the case when the magneto-conductivity demonstrates the regular behavior (I.7) under the simple condition  $\omega_B \tau \gg 1$ .

The corresponding magneto-resistance tensor can be written here in the form

$$\begin{aligned} \rho_{kl} \simeq & \frac{m^*}{ne^2\tau} \begin{pmatrix} (\omega_B \tau)^2 & \omega_B \tau & \omega_B \tau \\ \omega_B \tau & * & * \\ \omega_B \tau & * & * \end{pmatrix} + \\ & + \frac{m^*}{ne^2\tau} \begin{pmatrix} 0 & * & * \\ * & 0 & * \\ * & * & 0 \end{pmatrix} (\omega_B \tau)^{-1} + \\ & + \frac{m^*}{ne^2\tau} \begin{pmatrix} * & * & * \\ * & * & * \\ * & * & * \end{pmatrix} (\omega_B \tau)^{-2} + \dots \quad (\text{II.4}) \end{aligned}$$

In particular, the behavior of the transverse resistivity ( $\mathbf{j} \perp \mathbf{B}$ ) demonstrates a regular quadratic law:

$$\rho_\perp \sim B^2 \cos^2 \varphi + \text{const} , \quad \omega_B \tau \gg 1 , \quad (\text{II.5})$$

where  $\varphi$  is the angle with the  $x$ -axis in our coordinate system.

The situation is rather different in the case when the open trajectories have an irrational mean direction

$$\hat{d} \sim \mathbf{q}_1 + \kappa \mathbf{q}_2 , \quad \kappa \notin \mathbb{Q} \quad (\text{II.6})$$

in the plane  $\Gamma_\alpha$ . From one point of view, the limiting values of the conductivity tensor are also given here by the relations (I.8) in the limit  $\omega_B \tau \rightarrow \infty$ . At the same



time, the regular series (I.7), (II.4) can not be written in general for generic mean direction of the open trajectories. It can be shown also that the asymptotic behavior of the values  $\sigma^{kl}(B)$  demonstrates here a slower (irregular) approach to their limiting values  $\bar{\sigma}_{\infty}^{kl}(\mathbf{B}/B)$ . In general, the asymptotic behavior of  $\sigma^{kl}(B)$  inside  $\Omega_{\alpha}$  for irrational mean direction of the open trajectories can be represented in the form:

$$\sigma^{kl}(B) = \begin{pmatrix} a^2(B) & b(B) & c(B) \\ -b(B) & \bar{\sigma}_{\infty}^{22} + q^2(B) & \bar{\sigma}_{\infty}^{23} + r(B) \\ -c(B) & \bar{\sigma}_{\infty}^{23} - r(B) & \bar{\sigma}_{\infty}^{33} + p^2(B) \end{pmatrix}, \quad (\text{II.7})$$

where the functions  $a(B)$ ,  $b(B)$ ,  $c(B)$  have the following asymptotic behavior

$$a(B) \sim b(B) \sim c(B) \sim (\omega_B \tau)^{-1} \quad (\text{II.8})$$

At the same time, the functions  $q(B)$ ,  $p(B)$  have the following ‘‘general trend’’

$$q(B) \sim p(B) \sim \frac{\ln \omega_B \tau}{\omega_B \tau} \quad (\text{II.9})$$

Let us emphasize here that the relation  $\sim$  in (II.9) means just some general trend in the behavior of the corresponding functions which admits additional irregular corrections on the finite scales. In general, these corrections can be characterized as ‘‘cascades of step-like perturbations’’ with the structure defined by the properties of the number  $\kappa$  (Fig. 12). Let us note here that the behavior of  $q(B)$ ,  $p(B)$  can demonstrate noticeable local deviations from the trend for special irrational  $\kappa$  which can be approximated by rational numbers with a high precision. In particular, the last circumstance can be important for the directions of  $\mathbf{B}$  close to the special directions  $\mathbf{B}/B \in \gamma_{\mathbf{a}}^{\alpha}$  which were discussed above.

The behavior of the function  $r(B)$  is even more complicated compared with that of  $q(B)$  and  $p(B)$ . Here we would like to suggest just the following ‘‘reliable’’ restriction

$$|r(B)| \leq \frac{\ln \omega_B \tau}{\omega_B \tau} \quad (\text{II.10})$$

on the  $B$  - dependence of the function  $r(B)$  which can demonstrate rather irregular behavior at different values of  $B$ .

Another essential feature of the relations (II.9) - (II.10) is that the simple condition  $\omega_B \tau \gg 1$  is not sufficient here to get the values  $\bar{\sigma}_{\infty}^{kl}$  with a good precision. The latter circumstance can be understood from the fact that the values  $\bar{\sigma}_{\infty}^{kl}$  are given now by the averaging of certain dynamical values over a complicated part of the Fermi surface but not a one-dimensional circle. As a result, relations (II.9) - (II.10) can contain in fact a large dimensionless coefficient, determined by the geometry of the Fermi surface. We should expect then, that in the interval of not extremely high values of  $B$  the geometric characteristics of the carriers of open trajectories will

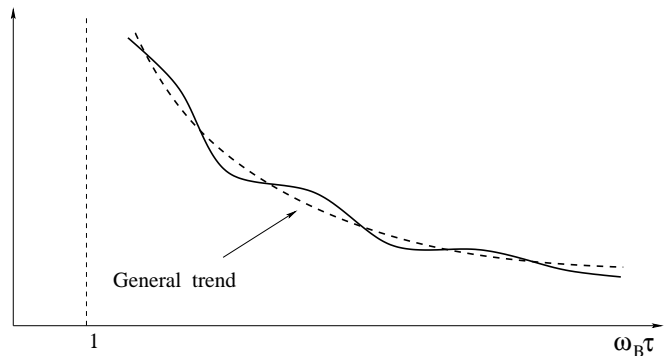


FIG. 12: The schematic sketch of the behavior of the functions  $q(B)$  and  $p(B)$  in the region  $\omega_B \tau \gg 1$ .

play important role in the behavior of  $\sigma^{kl}(B)$  and can give noticeable deviations from the asymptotic regime (II.9). As a consequence, we should expect also that in the interval of not extremely strong magnetic fields the interplay between the limiting values of  $\sigma^{kl}(B)$  and the corrections depending on  $B$  will play an essential role in conductivity behavior.

In general, the picture described above demonstrates the main features of the behavior of  $\sigma^{kl}(B)$  inside the mathematical Stability Zones  $\Omega_{\alpha}$ .

In the Zone  $\Lambda_{\alpha}$  we have to introduce the function  $\lambda(\mathbf{B}/B)$ ,  $1 \leq \lambda < \infty$ , characterizing the mean size of long closed trajectories for generic directions of  $\mathbf{B}$ . In common, the function  $\lambda(\mathbf{B}/B)$  can be defined as the ratio of the length of such trajectories in the  $\mathbf{p}$  - space to the size of the Brillouin zone. Let us note that the definition of the function  $\lambda(\mathbf{B}/B)$  has actually rather approximate character. It is natural then to introduce the ‘‘intermediate’’ stable values of conductivity  $\bar{\sigma}_{int}^{kl}(\mathbf{B}/B)$ , ( $k, l = 2, 3$ ), which are proportional to the measure of the long closed trajectories on the Fermi surface. For the behavior of conductivity for not extremely strong magnetic fields  $1 \ll \omega_B \tau < \lambda(\mathbf{B}/B)$  and generic directions of  $\mathbf{B}$  in  $\Lambda_{\alpha}$  we can then use the following relations

$$\sigma^{kl}(B) = \begin{pmatrix} a^2(B) & b(B) & c(B) \\ -b(B) & \bar{\sigma}_{int}^{22} + q^2(B) & \bar{\sigma}_{int}^{23} + r(B) \\ -c(B) & \bar{\sigma}_{int}^{23} - r(B) & \bar{\sigma}_{int}^{33} + p^2(B) \end{pmatrix} \quad (\text{II.11})$$

( $1 \ll \omega_B \tau < \lambda$ ), with the same remarks about the functions  $a(B)$ ,  $b(B)$ ,  $c(B)$ ,  $q(B)$ ,  $r(B)$ ,  $p(B)$ .

To describe the asymptotic behavior of conductivity in the region of extremely strong magnetic fields  $\omega_B \tau \gg \lambda(\mathbf{B}/B)$  for the same directions of  $\mathbf{B}$  it is convenient to consider separately the symmetric  $s^{kl}(B)$  and the anti-symmetric part  $a^{kl}(B)$  of the tensor  $\sigma^{kl}(B)$ . As will be shown below, the corresponding parts of  $\sigma^{kl}(B)$

can be approximated here by the following expressions

$$s^{kl}(B) \simeq \begin{pmatrix} 0 & 0 & 0 \\ 0 & 0 & 0 \\ 0 & 0 & \sigma'^{33} \end{pmatrix} + \frac{ne^2\tau}{m^*} \begin{pmatrix} (\omega_B\tau)^{-2} & \lambda(\omega_B\tau)^{-2} & \lambda(\omega_B\tau)^{-2} \\ \lambda(\omega_B\tau)^{-2} & \lambda^2(\omega_B\tau)^{-2} & \lambda^2(\omega_B\tau)^{-2} \\ \lambda(\omega_B\tau)^{-2} & \lambda^2(\omega_B\tau)^{-2} & \lambda^2(\omega_B\tau)^{-2} \end{pmatrix}, \quad (\text{II.12})$$

where

$$\sigma'^{33} < \bar{\sigma}_{int}^{33}, \quad (\text{II.13})$$

and

$$a^{kl}(B) \simeq \frac{ne^2\tau}{m^*} \begin{pmatrix} 0 & (\omega_B\tau)^{-1} & (\omega_B\tau)^{-1} \\ (\omega_B\tau)^{-1} & 0 & (\omega_B\tau)^{-1} \\ (\omega_B\tau)^{-1} & (\omega_B\tau)^{-1} & 0 \end{pmatrix}, \quad (\text{II.14})$$

respectively.

Let us note, that the interplay between the symmetric and the anti-symmetric parts of  $\sigma^{kl}(B)$  has here rather nontrivial character. Thus, we can see that the values  $\sigma^{23}(B)$  and  $\sigma^{32}(B)$  are defined mostly by the symmetric part in the interval

$$\lambda(\mathbf{B}/B) \leq \omega_B\tau \leq \lambda^2(\mathbf{B}/B),$$

and by the anti-symmetric part for  $\omega_B\tau > \lambda^2(\mathbf{B}/B)$ . Another important feature in the behavior of conductivity is given here by the relation (II.13), which indicates the suppression of the conductivity along the direction of  $\mathbf{B}$  in the region  $\omega_B\tau \gg \lambda(\mathbf{B}/B) \gg 1$ .

The values of  $\lambda(\mathbf{B}/B)$  are equal to 1 on the exterior boundary of the region  $\Lambda_\alpha$ . At the same time, we should put  $\lambda(\mathbf{B}/B) = \infty$  on the curves  $\hat{\gamma}_\alpha$  in  $\Lambda_\alpha$  and on the boundary between the regions  $\Omega_\alpha$  and  $\Lambda_\alpha$ . It's not difficult to see that the functions  $\bar{\sigma}_{int}^{kl}(\mathbf{B}/B)$  lose their sense and are not well defined on the exterior boundary of  $\Lambda_\alpha$ . At the same time, we can write  $\bar{\sigma}_{int}^{kl}(\mathbf{B}/B) = \bar{\sigma}_{\infty+}^{kl}(\mathbf{B}/B)$ , where  $\bar{\sigma}_{\infty+}^{kl}(\mathbf{B}/B)$  are the boundary values of  $\bar{\sigma}_{\infty}^{kl}(\mathbf{B}/B)$  inside  $\Omega_\alpha$ , on the boundary between  $\Omega_\alpha$  and  $\Lambda_\alpha$ .

According to the above remarks, we can see actually, that the exact boundary between the regions  $\Omega_\alpha$  and  $\Lambda_\alpha$  is not usually observable in experiments.

We can see that the picture described above makes the analytic structure of tensor  $\sigma^{kl}(\mathbf{B})$  in the Zone  $\hat{\Omega}_\alpha$  rather complicated. The most complicated situation can arise in that part of the Zone  $\Lambda_\alpha$  where we have the relation  $\omega_B\tau \simeq \lambda(\mathbf{B}/B)$  for typical values of  $B$  in the experiment. In the last case the behavior of  $\sigma^{kl}(B)$  can demonstrate the most complicated trends, which are intermediate between (II.11) and (II.12) - (II.14). In experimental study of the behavior of conductivity it can be convenient to approximate the corresponding regimes

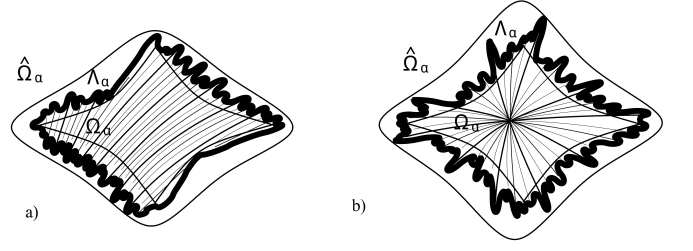


FIG. 13: The Zone of the most complicated behavior of conductivity tensor (black) in the “experimentally observable Stability Zone”  $\hat{\Omega}_\alpha$ .

with the aid of intermediate powers of  $\omega_B\tau$  and write

$$\sigma^{kl}(B) \simeq \frac{ne^2\tau}{m^*} \begin{pmatrix} (\omega_B\tau)^{-2} & (\omega_B\tau)^{-1} & (\omega_B\tau)^{-1} \\ (\omega_B\tau)^{-1} & (\omega_B\tau)^{-2\mu} & (\omega_B\tau)^{-\nu} \\ (\omega_B\tau)^{-1} & (\omega_B\tau)^{-\nu} & * \end{pmatrix}$$

( $0 \leq \mu, \nu \leq 1$ ,  $\mu \simeq \nu$ ) in the intervals of rather high values of  $B$ .

As an example, putting approximately  $\mu = \nu$ , we can write the relation for the resistivity behavior in strong magnetic fields:

$$\rho_{kl}(B) \simeq \frac{m^*}{ne^2\tau} \begin{pmatrix} (\omega_B\tau)^{2-2\mu} & \omega_B\tau & (\omega_B\tau)^{1-\mu} \\ \omega_B\tau & * & * \\ (\omega_B\tau)^{1-\mu} & * & * \end{pmatrix}$$

In particular, we get the following approximation for the resistivity in the plane orthogonal to  $\mathbf{B}$ :

$$\rho_\perp \sim B^{2-2\mu} \cos^2\varphi + \text{const}, \quad \omega_B\tau \gg 1,$$

where  $\varphi$  is the angle with the  $x$ -axis in our coordinate system.

We should say, however, that the powers  $\mu$  and  $\nu$  play here just the role of local approximating parameters and are unstable both with respect to rotations of  $\mathbf{B}$  and big changes of its absolute value. Let us note also that the corresponding part of  $\Lambda_\alpha$  has in general rather complicated structure view the complicated behavior of the function  $\lambda(\mathbf{B}/B)$  (Fig. 13).

We can see then that the experimental study of galvano-magnetic phenomena in the presence of open trajectories can reveal rather non-trivial behavior of magneto-conductivity, which is caused both by the complicated dependence of conductivity on the value of  $B$  and possible small variations of directions of  $\mathbf{B}$  in experiment. The general analytical picture described above can be used for description of the dependence of the magneto-conductivity both on the value of  $B$  and the direction of  $\mathbf{B}$  inside the “experimentally observable” Stability Zone  $\hat{\Omega}_\alpha$ . Let us say again that the picture described above is based just on geometric consideration of the trajectories of system (I.1) and does not include many other essential effects which can be important in real metals.

At the end of this section, we would like to note that the picture described above is based on the assumption that the Fermi surface of a metal has a complicated form. This assumption means, in particular, that the carriers of the stable open trajectories have the form defined by general topological theorems for generic dispersion law. This form will be described in the next section and has some special features for generic Fermi surfaces  $S_F$ . However, for special simple Fermi surfaces the carriers of open trajectories can have much simpler form, which will result also in simpler behavior of conductivity in comparison with the described above.

As an example of the simple Fermi surface, we can consider just a pair of slightly deformed integral planes in the  $\mathbf{p}$  - space (like for some classes of organic metals). It is easy to see that the exact mathematical Stability Zone  $\Omega$  can be identified here with the whole sphere  $\mathbb{S}^2$  and coincides with the “experimentally observable” Stability Zone  $\hat{\Omega}$ . As a result, we can not observe here the effects, connected with the reconstruction of the open trajectories, typical for the Zones  $\Lambda_\alpha$ . The “rational peaks” in the conductivity can be observable here for the surfaces having essential deformations (see e.g. [30]), however, they decrease exponentially with the growth of the numbers  $(m_1, m_2, m_3)$ . As a result, we can expect here the experimental evidence of just a finite number of the lines  $\gamma_{\mathbf{a}}$  instead of the complicated angle dependence of conductivity, observable in the Zones  $\Omega_\alpha$ . It is easy to see also, that for the case of vanishing amplitude of deformation of the planes the conductivity tensor demonstrates just a very fast approach to its limiting form given by formula (I.8).

In the next sections we will make more detailed consideration of the effects described above using the kinetic approach to the transport phenomena. In general, all the statements above can be obtained within the  $\tau$  - approximation for the kinetic equation for the electron gas.

### III. THE GEOMETRY OF THE STABLE OPEN TRAJECTORIES AND THE CONDUCTIVITY TENSOR.

Let us start with the description of generic picture arising on the Fermi surface in the case of presence of the stable open trajectories at  $\epsilon = \epsilon_F$  ([10]). Everywhere below we will assume that the Fermi surface represents a smooth non-selfintersecting 3-periodic surface in  $\mathbf{p}$  - space.

Consider the general picture of intersection of a 3-periodic surface in  $\mathbf{p}$  - space by the planes orthogonal to  $\mathbf{B}$  (Fig. 3). First, let us look at the closed trajectories in  $\mathbf{p}$  - space if they present on the Fermi surface.

The non-singular closed trajectories in  $\mathbf{p}$  - space are always locally stable and can be combined into connected cylinders consisting of trajectories of this type. In the case when a connected component of the Fermi surface

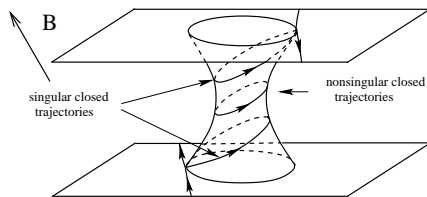


FIG. 14: A part of the Fermi surface representing a cylinder of closed trajectories bounded by singular trajectories.

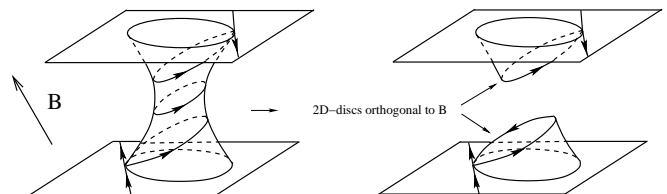


FIG. 15: The reconstruction of the Fermi surface given by elimination of nonsingular closed trajectories and filling the holes by the discs orthogonal to  $\mathbf{B}$ .

does not consist of the closed trajectories only, these cylinders have finite heights and are bounded by singular closed trajectories (Fig. 14).

Let us make now the following reconstruction of the Fermi surface:

We remove all the cylinders of closed trajectories from the Fermi surface and fill the created holes by 2-dimensional discs orthogonal to  $\mathbf{B}$  (Fig. 15).

It is easy to see that the reconstructed Fermi surface carries the same open electron trajectories as the initial one, so we can investigate the behavior of open trajectories on the reconstructed surface.

The reconstructed Fermi surface represents a 3-periodic surface which contains in general infinitely many connected components in  $\mathbf{p}$  - space. One important theorem can be formulated about the connected components of the reconstructed Fermi surface in the case of presence of stable open trajectories ([8, 10, 36]):

Every connected component of the reconstructed Fermi surface carrying open electron trajectories represents a periodic deformation of an integral plane in  $\mathbf{p}$  - space.

Let us remind here that the plane  $\Gamma$  is called integral if it is generated by any two reciprocal lattice vectors. So, every connected component of the reconstructed Fermi surface has two independent periods represented by two vectors of the reciprocal lattice. Let us note also that the picture described above is evidently stable with respect to all small rotations of  $\mathbf{B}$  view the local stability of nonsingular closed trajectories on the Fermi surface.

All the connected components of the reconstructed Fermi surface are parallel to each other which leads to

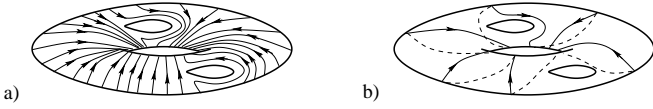


FIG. 16: Schematic topological description of the dense (non-periodic) trajectory on  $\mathbb{T}^2 \setminus \cup D_i^2$  and closed (periodic in  $\mathbf{p}$ -space) trajectory on the same manifold after the factorization over the reciprocal lattice vectors.

the coinciding of the mean directions of all stable open trajectories in  $\mathbf{p}$ -space. The last property was called in [25, 26] the Topological Resonance and plays very important role in the experimental observation of the anisotropic regimes of conductivity behavior and of the Topological Numbers corresponding to a given Stability Zone.

In this paper we will use the picture described above as the general picture arising in the case of presence of stable non-closed electron trajectories on the Fermi surface. Let us note here that this picture can have some additional features for some special directions of  $\mathbf{B}$  within the Stability Zone (see [10]) which can be also detected from the experimental point of view ([25, 26]). These phenomena, however, have a non-generic character and will not be considered here.

After the factorization over the vectors of the reciprocal lattice every connected component of the reconstructed Fermi surface becomes a two-dimensional torus  $\mathbb{T}^2$  embedded in  $\mathbb{T}^3$ . The number of non-equivalent components in  $\mathbb{T}^3$  is always finite and represents an even number.

The open (in  $\mathbf{p}$ -space) trajectories of system (I.1) on the Fermi level are given by the intersections of the components of the reconstructed Fermi surface with the planes orthogonal to  $\mathbf{B}$  and represent irrational coverings of the corresponding tori  $\mathbb{T}^2$  (except the discs  $D^2$ ) in generic situation (Fig. 16 a). However, for special directions of  $\mathbf{B}$  the intersection of the plane orthogonal to  $\mathbf{B}$  with the integral plane  $\Gamma_\alpha$  ( $\mathbf{B} \in \Omega_\alpha$ ) can have rational (integral) direction, which means in fact that the corresponding trajectories of (I.1) become periodic in  $\mathbf{p}$ -space. The corresponding trajectories in  $\mathbb{T}^3$  become now closed curves on the tori  $\mathbb{T}^2$  and are not dense anymore on the sets  $\mathbb{T}^2 \setminus \cup D_i^2$ , which can be called the “carriers of open trajectories” on the Fermi surface (Fig. 16 b).

As we can see, the generic and the periodic open trajectories demonstrate an obvious difference in their statistical properties on the “carriers of open trajectories”. As will see below, this circumstance will play important role for the behavior of the conductivity tensor  $\sigma^{kl}(\mathbf{B})$  in the limit  $\omega_B \tau \rightarrow \infty$ .

We can see here that the periodic trajectories can not appear for completely irrational directions of  $\mathbf{B}$  since the plane orthogonal to  $\mathbf{B}$  should contain at least one vector of the reciprocal lattice, giving the mean direction of such trajectories. Let us note that the class of rationality of a

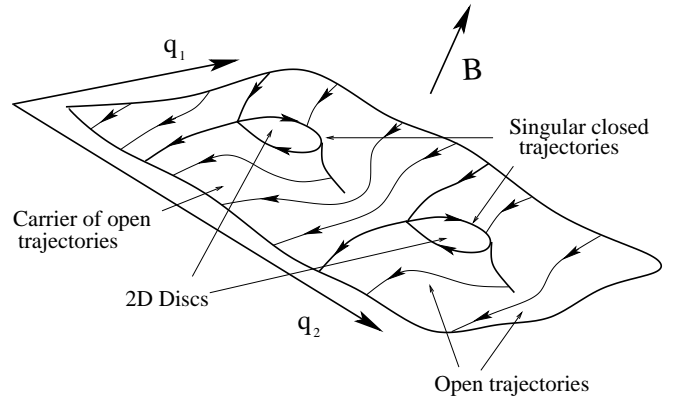


FIG. 17: The connected component of the reconstructed Fermi surface representing a periodically deformed integral plane in  $\mathbf{p}$ -space with periods  $\mathbf{q}_1, \mathbf{q}_2 \in L^*$ .

direction of magnetic field  $\mathbf{B}$  is defined as the number of linearly independent reciprocal lattice vectors lying in the plane orthogonal to  $\mathbf{B}$ . In particular, the direction  $\hat{\mathbf{B}}_\alpha^0$ , orthogonal to the plane  $\Gamma_\alpha$ , represents a purely rational direction according to this definition.

In general, it is not difficult to see that the directions of  $\mathbf{B}$  in a Stability Zone  $\Omega_\alpha$ , corresponding to periodic open trajectories, form a dense net of one-dimensional curves, which do not intersect each other in  $\Omega_\alpha$  in the case when the direction  $\hat{\mathbf{B}}_\alpha^0 \perp \Gamma_\alpha$  does not belong to  $\Omega_\alpha$  (Fig. 9 a) or all intersect at the point  $\hat{\mathbf{B}}_\alpha^0$  if  $\hat{\mathbf{B}}_\alpha^0 \in \Omega_\alpha$  (Fig. 9 b).

As we already said above, all the one-dimensional curves  $\gamma_a^\alpha$  should be actually extended outside the Stability Zone  $\Omega_\alpha$  since the periodic open trajectories exist in fact for a wider set of directions of  $\mathbf{B}$  surrounding  $\Omega_\alpha$ . The periodic open trajectories become unstable with respect to small rotations of  $\mathbf{B}$  outside  $\Omega_\alpha$ . We have to note also that the difference between the curves  $\gamma_a^\alpha$  and  $\hat{\gamma}_a^\alpha$  decreases with increasing of the “denominator” of a rational mean direction of the periodic trajectories and vanishes in the limit  $|\mathbf{a}| \rightarrow \infty$  (Fig. 10).

Let us consider now the carriers of open trajectories in more detail.

The general form of connected components of the reconstructed Fermi surface is shown at Fig. 17 and represents a periodically deformed integral plane in  $\mathbf{p}$ -space with two periods  $\mathbf{q}_1, \mathbf{q}_2$ , given by two independent reciprocal lattice vectors.

The carriers of open trajectories in  $\mathbf{p}$ -space represent the same periodically deformed integral planes without “artificial” two-dimensional discs  $D^2$ , attached after the removal of closed trajectories. Let us exclude here the non-generic case when the magnetic field  $\mathbf{B}$  is orthogonal to the plane  $\Gamma_\alpha$  and consider the generic case

$$\mathbf{B} \nparallel [\mathbf{q}_1 \times \mathbf{q}_2] \quad (\text{III.1})$$

We will assume in our considerations that the  $z$  - axis is always chosen along the direction of  $\mathbf{B}$  while the  $x$  - and  $y$  - axis are orthogonal to  $\mathbf{B}$ . In the generic situation described above the values of  $p_z$  separate all different trajectories at a given component and  $p_z$  can be chosen as a “coordinate” on the corresponding carrier of open trajectories.

The second coordinate on the carriers of open trajectories is naturally given by the parameter  $t$ , measured along the trajectories according to system (I.1).

In general, a natural system of local coordinates in  $\mathbf{p}$  - space (or  $\mathbb{T}^3$ ) is given by the triple  $(p_z, t, \epsilon)$  if we consider system (I.1) for all values of  $\epsilon$ . The coordinates  $(p_z, t, \epsilon)$  are naturally connected with system (I.1) and possess also one more remarkable property:

$$dp_z dt d\epsilon \equiv \frac{c}{eB} dp_x dp_y dp_z \quad (\text{III.2})$$

The last property is caused in fact by the Hamiltonian properties of system (I.1), which can be considered as a Hamiltonian system with the Hamiltonian  $\epsilon(\mathbf{p})$  and the Poisson bracket

$$\{p_1, p_2\} = \frac{e}{c} B, \quad \{p_2, p_3\} = 0, \quad \{p_3, p_1\} = 0$$

( $\mathbf{B} \parallel \nabla z$ ).

It can be seen also that the integration over the layer restricted by the energy values  $\epsilon_0$  and  $\epsilon_0 + d\epsilon$  can be represented by the integration over the energy surface  $\epsilon(\mathbf{p}) = \epsilon_0$  according to the formula

$$\begin{aligned} \iiint_{\epsilon_0 < \epsilon(\mathbf{p}) < \epsilon_0 + d\epsilon} f(p_x, p_y, p_z) dp_x dp_y dp_z &= \\ = \frac{eB d\epsilon}{c} \iint_{\epsilon(\mathbf{p}) = \epsilon_0} f(p_z, t, \epsilon_0) dp_z dt & \quad (\text{III.3}) \end{aligned}$$

Formula (III.3) gives in fact very convenient way of statistical averaging of any value over the Fermi distribution in presence of magnetic field.

It's not difficult to see that every connected component of the reconstructed Fermi surface can be divided into a periodic set of the fundamental (minimal) domains identical to each other (Fig. 18).

It can be seen also that the fundamental domains can be chosen in the form of “curvilinear” parallelograms with the sides, corresponding to the vectors  $\mathbf{q}_1$  and  $\mathbf{q}_2$ . The division of the connected components of the reconstructed Fermi surface gives also a natural division of the corresponding carriers of open trajectories into fundamental domains.

All the fundamental domains are physically equivalent to each other, so every domain represents in fact the full set of the physical states represented by the whole component. The two-dimensional tori  $\mathbb{T}^2 \subset \mathbb{T}^3$ , which we discussed above, can be considered also as any of the fundamental domains with the identified opposite sides. As we said already, every nonsingular open trajectory becomes then a smooth curve on the torus  $\mathbb{T}^2$  which can

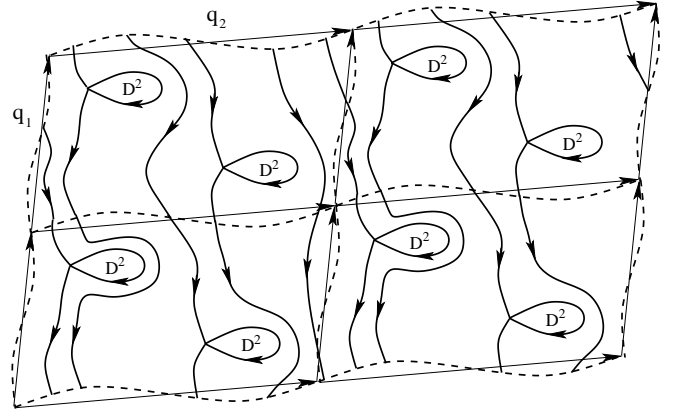


FIG. 18: The periodic set of the fundamental domains on a connected component of the reconstructed Fermi surface.

be open or closed (periodic in  $\mathbf{p}$  - space) depending on the direction of  $\mathbf{B}$  (Fig. 16).

The difference between the closed and the non-closed trajectories on the tori  $\mathbb{T}^2$  causes an evident difference in the averaging of any of the physical quantities over time on the trajectories of this kind. Thus, we can claim that any time average over generic (non-closed on  $\mathbb{T}^2$ ) trajectory coincides with the averaging of the corresponding quantity over the carrier of open trajectories, which depends smoothly on the direction of  $\mathbf{B}$  inside the “Stability Zone”. On the other hand, the time average over a periodic (closed on  $\mathbb{T}^2$ ) trajectory is in general different from the mean value of the same quantity on the carrier of open trajectories. As can be seen, the last feature can lead to irregular dependence of the conductivity tensor on the direction of  $\mathbf{B}$  inside  $\Omega_\alpha$ .

Let us consider now the standard kinetic approach (see e.g. [1, 23, 35]) to the magneto-transport phenomena, using the geometric picture described above.

The full dynamical system for the adiabatic evolution of the electron states both in presence of magnetic and electric fields can be written as

$$\dot{\mathbf{p}} = \frac{e}{c} [\nabla\epsilon(\mathbf{p}) \times \mathbf{B}] + e\mathbf{E} \quad (\text{III.4})$$

In system (III.4) the electric field  $\mathbf{E}$  will be considered as a small value while the value of magnetic field is supposed to satisfy the strong magnetic field limit condition  $\omega_B \tau \gg 1$ .

In the kinetic approach we have to introduce the single-particle distribution function  $f(\mathbf{p}, t)$  satisfying the Boltzmann equation

$$\begin{aligned} f_t + \frac{e}{c} \sum_{l=1}^3 [\nabla\epsilon(\mathbf{p}) \times \mathbf{B}]^l \frac{\partial f}{\partial p^l} + e \sum_{l=1}^3 E^l \frac{\partial f}{\partial p^l} &= \\ = I[f](\mathbf{p}, t) \quad , & \quad (\text{III.5}) \end{aligned}$$

where  $I[f]$  represents the collision integral. Here we will

be interested in the stationary solutions of the equation (III.5), so we put now  $f(\mathbf{p}, t) = f(\mathbf{p})$ .

In the absence of electric field the distribution function  $f(\mathbf{p})$  is given by its equilibrium values

$$f_0(\mathbf{p}) = \frac{1}{\exp[(\epsilon(\mathbf{p}) - \epsilon_F)/T] + 1}$$

and we have identically  $I[f](\mathbf{p}) \equiv 0$ . The conductivity tensor  $\sigma^{kl}(\mathbf{B})$  is defined by the linear in  $\mathbf{E}$  correction to the function  $f_0(\mathbf{p})$ , satisfying the equation

$$\begin{aligned} \frac{e}{c} \sum_{l=1}^3 [\nabla\epsilon(\mathbf{p}) \times \mathbf{B}]^l \frac{\partial f_{(1)}}{\partial p^l} + e \sum_{l=1}^3 E^l \frac{\partial f_0}{\partial p^l} &= \\ &= \left[ \hat{L}_{[f_0]} \cdot f_{(1)} \right](\mathbf{p}) \quad , \quad (\text{III.6}) \end{aligned}$$

where  $\hat{L}_{[f_0]}$  is the linearization of the functional  $I[f](\mathbf{p})$  on the corresponding function  $f_0$ . The value  $\hat{L}_{[f_0]} \cdot f_{(1)}$  can be considered as a term, connected with the relaxation of non-equilibrium perturbations to the equilibrium state. In the so-called  $\tau$ -approximation the right-hand part of system (III.6) can be replaced by the value  $-f_{(1)}(\mathbf{p})/\tau$ , where  $\tau$  plays the role of the characteristic relaxation time. It will be convenient here to use the  $\tau$ -approximation for the equation (III.6), which is enough to catch all the main features of our consideration. The characteristic relaxation time  $\tau$  is usually identified with the mean free electron motion time.

Let us introduce now the variable  $s = teB/c$ , where  $t$  is the parameter along the trajectories of system (I.1), introduced above, and consider the coordinate system  $(p_z, s, \epsilon)$  in the  $\mathbf{p}$ -space. The parameter  $s$  has a purely geometrical meaning in  $\mathbf{p}$ -space and does not depend on the value of  $B$ . According to (III.2) - (III.3), we can naturally write

$$\begin{aligned} dp_z ds d\epsilon &\equiv dp_x dp_y dp_z \quad , \\ \iiint_{\epsilon_0 < \epsilon(\mathbf{p}) < \epsilon_0 + d\epsilon} f(p_x, p_y, p_z) dp_x dp_y dp_z &= \\ &= d\epsilon \iint_{\epsilon(\mathbf{p}) = \epsilon_0} f(p_z, s, \epsilon_0) dp_z ds \end{aligned}$$

It's not difficult to see also, that under our assumptions above the equation on the function  $f_{(1)}(p_z, s, \epsilon)$  can be represented as

$$\frac{eB}{c} \frac{\partial f_{(1)}}{\partial s} + e (\mathbf{E} \cdot \mathbf{v}_{gr}) \frac{\partial f_0}{\partial \epsilon} = -f_{(1)}/\tau$$

in the coordinate system  $(p_z, s, \epsilon)$ .

After the substitution

$$f_{(1)}(p_z, s, \epsilon) = -\frac{\partial f_0(\epsilon)}{\partial \epsilon} \sum_{l=1}^3 E^l g^l(p_z, s, \epsilon) \quad (\text{III.7})$$

we get the linear systems

$$\frac{eB}{c} \frac{\partial g^l}{\partial s} - e v_{gr}^l(p_z, s, \epsilon) = -\frac{1}{\tau} g^l \quad (\text{III.8})$$

for the functions  $g^l(p_z, s, \epsilon)$ .

The solutions of systems (III.8) which we need can be written in the form

$$g^l(p_z, s, \epsilon) = \frac{c}{B} \int_{-\infty}^s v_{gr}^l(p_z, s', \epsilon) e^{\frac{c(s'-s)}{eB\tau}} ds' \quad , \quad (\text{III.9})$$

where the integration is taken along the whole part of a trajectory preceding the point  $(p_z, s, \epsilon)$ .

The mean value of the density of the electric current is given by the formula

$$j^k = e \int v_{gr}^k(p_z, s, \epsilon) f_{(1)}(p_z, s, \epsilon) \frac{dp_z ds d\epsilon}{(2\pi\hbar)^3}$$

(in the linear approximation in  $E$ ).

The form (III.7) of the correction  $f_{(1)}$  gives in fact very strong concentration of  $f_{(1)}(p_z, s, \epsilon)$  near the Fermi surface for most of the normal metals, so the term  $-\partial f_0/\partial \epsilon$  can be actually replaced by the delta-function  $\delta(\epsilon - \epsilon_F)$  in the integration over  $\epsilon$ . Finally, we come to the following simple expression for the value of the electric current density:

$$\begin{aligned} j^k &= \frac{ec}{B} \iint_{S_F} \frac{dp_z ds}{(2\pi\hbar)^3} v_{gr}^k(p_z, s) \times \\ &\times \sum_{l=1}^3 \int_{-\infty}^s v_{gr}^l(p_z, s') e^{\frac{c(s'-s)}{eB\tau}} ds' E^l \end{aligned}$$

The general form of the conductivity tensor  $\sigma^{kl}$  can be represented as

$$\begin{aligned} \sigma^{kl}(B) &= \frac{ec}{B} \iint_{S_F} \frac{dp_z ds}{(2\pi\hbar)^3} v_{gr}^k(p_z, s) \times \\ &\times \int_{-\infty}^s v_{gr}^l(p_z, s') e^{\frac{c(s'-s)}{eB\tau}} ds' \quad (\text{III.10}) \end{aligned}$$

At the same time, the contribution of the open trajectories  $\Delta\sigma^{kl}$  is given by the restriction of the integral in (III.10) to the set of the carriers of open trajectories  $\hat{S}_F$  instead of the whole Fermi surface, so we can write:

$$\begin{aligned} \Delta\sigma^{kl}(B) &= \frac{ec}{B} \iint_{\hat{S}_F} \frac{dp_z ds}{(2\pi\hbar)^3} v_{gr}^k(p_z, s) \times \\ &\times \int_{-\infty}^s v_{gr}^l(p_z, s') e^{\frac{c(s'-s)}{eB\tau}} ds' \quad (\text{III.11}) \end{aligned}$$

Let us say, that the irregular behavior of  $\sigma^{kl}(\mathbf{B})$  in  $\Omega_\alpha$  is completely determined by the functions  $\Delta\sigma^{kl}(\mathbf{B})$ , so we will be interested here mostly in the behavior of  $\Delta\sigma^{kl}(\mathbf{B})$  in the limit  $B \rightarrow \infty$ .

It's not difficult to see that for all types of trajectories in our case we can write in the limit  $B \rightarrow \infty$  for the conductivity tensor

$$\sigma_{\infty}^{kl} = e^2 \tau \iint_{S_F} v_{gr}^k(p_z, s) \langle v_{gr}^l \rangle_{tr}(p_z, s) \frac{dp_z ds}{(2\pi\hbar)^3},$$

where  $\langle v_{gr}^l \rangle_{tr}(p_z, s)$  is the mean value of the group velocity component on the trajectory passing through the point  $(p_z, s)$ :

$$\langle v_{gr}^l \rangle_{tr}(p_z, s) = \lim_{s_0 \rightarrow \infty} \frac{1}{s_0} \int_{s-s_0}^s v_{gr}^l(p_z, s') ds'$$

To get the contribution of the open trajectories we have now to restrict the integration to the set of the carriers of open trajectories  $\hat{S}_F$  on the Fermi surface, so we can write for the contribution of the stable open trajectories to the conductivity in the limit  $B \rightarrow \infty$ :

$$\Delta \sigma_{\infty}^{kl} = e^2 \tau \iint_{\hat{S}_F} v_{gr}^k(p_z, s) \langle v_{gr}^l \rangle_{tr}(p_z, s) \frac{dp_z ds}{(2\pi\hbar)^3}$$

Let us note here that according to our choice of coordinate system  $(x, y, z)$  we will always have  $\langle v_{gr}^x \rangle_{tr} = 0$  and  $\langle v_{gr}^y \rangle_{tr} \neq 0$ ,  $\langle v_{gr}^z \rangle_{tr} \neq 0$  for the stable open trajectories.

We can see also, that according to the definition above, the values  $\langle v_{gr}^k \rangle_{tr}(p_z, s)$  do not depend in fact on the variable  $s$  for the trajectories of our type. As a corollary, the first multiplier can be also replaced by its mean value on every trajectory of system (I.1). Finally, we can write for the contribution of the stable open trajectories to the magneto-conductivity for  $B \rightarrow \infty$ :

$$\Delta \sigma_{\infty}^{kl} = e^2 \tau \iint_{\hat{S}_F} \langle v_{gr}^k \rangle_{tr}(p_z) \langle v_{gr}^l \rangle_{tr}(p_z) \frac{dp_z ds}{(2\pi\hbar)^3} \quad (\text{III.12})$$

Let us note that the tensor  $\sigma_{\infty}^{kl}$  is purely symmetric according to (III.12), which is not the case for finite values of  $B$ .

Let us give now qualitative derivation of the regimes of the conductivity behavior described in the previous section.

As it is not difficult to see, in the case of generic direction of  $\mathbf{B}$  (non-periodic open trajectories) the mean values  $\langle v_{gr}^k \rangle_{tr}(p_z)$  can be identified with the mean values of the same quantities on the corresponding (connected) carrier of open trajectories  $\hat{S}_F^{\gamma}$ :

$$\langle v_{gr}^k \rangle_{\hat{S}_F^{\gamma}} = \iint_{\hat{S}_F^{\gamma}} v_{gr}^k(p_z, s) dp_z ds / \iint_{\hat{S}_F^{\gamma}} dp_z ds$$

and are constant on each carrier of the stable open trajectories.

In general, the mean values  $\langle v_{gr}^k \rangle_{\hat{S}_F^{\gamma}}$  can be also expressed through the values  $\langle v_{gr}^k \rangle_{tr}(p_z)$  by the formula

$$\langle v_{gr}^k \rangle_{\hat{S}_F^{\gamma}} = \iint_{\hat{S}_F^{\gamma}} \langle v_{gr}^k \rangle_{tr}(p_z) dp_z ds / \iint_{\hat{S}_F^{\gamma}} dp_z ds \quad (\text{III.13})$$

Let us introduce now the functions

$$\Delta \bar{\sigma}_{\infty}^{kl}(\mathbf{B}/B) = e^2 \tau \sum_{\gamma} \iint_{\hat{S}_F^{\gamma}} \langle v_{gr}^k \rangle_{\hat{S}_F^{\gamma}} \langle v_{gr}^l \rangle_{\hat{S}_F^{\gamma}} \frac{dp_z ds}{(2\pi\hbar)^3}$$

where the summation is taken over all the connected carriers  $\hat{S}_F^{\gamma}$  of the stable open trajectories.

The functions  $\Delta \bar{\sigma}_{\infty}^{kl}(\mathbf{B}/B)$  are smooth functions of the direction of  $\mathbf{B}$  inside any Stability Zone  $\Omega_{\alpha}$ . According to (III.12), the functions  $\Delta \bar{\sigma}_{\infty}^{kl}(\mathbf{B}/B)$  coincide with the limiting values  $\Delta \sigma_{\infty}^{kl}(\mathbf{B}/B)$  for generic directions of  $\mathbf{B}$ , corresponding to non-periodic form of the open trajectories.

At the same time, for special directions of  $\mathbf{B}$ , corresponding to the periodic form of the stable open trajectories, the values (III.12) do not coincide with  $\Delta \bar{\sigma}_{\infty}^{kl}(\mathbf{B}/B)$  due to the dependence of the values  $\langle v_{gr}^k \rangle_{tr}(p_z)$  on  $p_z$ . Just from the Schwartz inequality we can write in this case

$$\Delta \sigma_{\infty}^{22}(\mathbf{B}/B) - \Delta \bar{\sigma}_{\infty}^{22}(\mathbf{B}/B) > 0,$$

$$\Delta \sigma_{\infty}^{33}(\mathbf{B}/B) - \Delta \bar{\sigma}_{\infty}^{33}(\mathbf{B}/B) > 0$$

as it was written above. The values

$$\Delta \sigma_{\infty}^{kl}(\mathbf{B}/B) - \Delta \bar{\sigma}_{\infty}^{kl}(\mathbf{B}/B), \quad k \neq l,$$

can have in general arbitrary signs. We have also  $\Delta \sigma_{\infty}^{kl}(\mathbf{B}/B) = \Delta \bar{\sigma}_{\infty}^{kl}(\mathbf{B}/B) = 0$ , if  $k$  or  $l$  is equal to 1, in our coordinate system.

Let us point out an important role of the geometry of the carriers of open trajectories on the complicated Fermi surfaces for the effect which we discuss here. As it is not difficult to see, the difference  $\Delta \sigma_{\infty}^{kl}(\mathbf{B}/B) - \Delta \bar{\sigma}_{\infty}^{kl}(\mathbf{B}/B)$  is defined actually by the ‘‘inconstancy’’ of the functions  $\langle v_{gr}^k \rangle_{tr}(p_z)$  on the carriers of the stable open trajectories. As can be seen at Fig. 19, the presence of the singular trajectories on the carriers of open trajectories makes the behavior of  $\langle v_{gr}^k \rangle_{tr}(p_z)$  rather irregular in the case of periodicity of the open trajectories on the Fermi surface. Thus, the periodic trajectories adjacent to the singular trajectory from different sides have rather different geometry in  $\mathbf{p}$ -space. As a result, we can expect that the mean variations of the values  $\langle v_{gr}^k \rangle_{tr}(p_z)$  on the carrier of open trajectories can be comparable with the mean values of the same quantities and the same can be stated also about the difference  $\Delta \sigma_{\infty}^{kl}(\mathbf{B}/B) - \Delta \bar{\sigma}_{\infty}^{kl}(\mathbf{B}/B)$ ,  $(k, l = 2, 3)$ . It should be also noted here, however, that this effect decreases with increasing of ‘‘denominators’’ of the rational mean direction of the open trajectories due to the increasing of the density of the periodic open trajectory on a carrier of open trajectories. As we also said already, we have the identities  $\langle v_{gr}^x \rangle_{tr} \equiv 0$  in our coordinate system.

To evaluate the dependence of  $\Delta \sigma_{\infty}^{kl}(\mathbf{B}/B) - \Delta \bar{\sigma}_{\infty}^{kl}(\mathbf{B}/B)$  on the numbers  $(k_1, k_2)$  it is convenient to choose the fundamental domain on the carrier of open

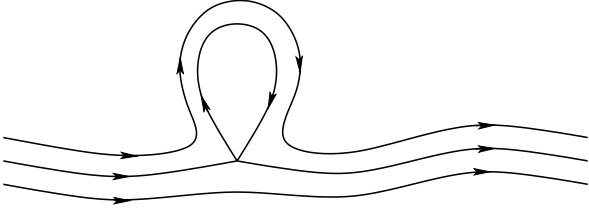


FIG. 19: Open periodic trajectories with rather different geometry near the singular trajectory on the Fermi surface.

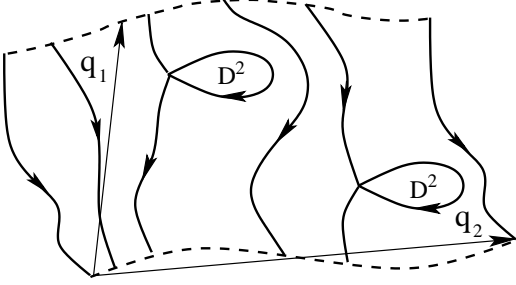


FIG. 20: The fundamental domain on the carrier of open trajectories having the form of curvilinear parallelogram with two opposite sides, represented by two equivalent parts of open electron trajectories.

trajectories in the form of curvilinear parallelogram with two opposite sides, represented by two equivalent parts of periodic open trajectories (Fig. 20).

The values  $p_z$  and  $s$  give a good parametrization of the fundamental domain under the requirement (III.1). We can assume without loss of generality that  $\mathbf{B}$  is not orthogonal to the vector  $\mathbf{q}_2$  which will also mean that the mean direction of the open trajectories does not coincide with the direction of  $\mathbf{q}_2$ . Let us put also that the values of  $p_z$  belong to the interval  $[0, p_z^0]$  for our fundamental domain, where  $p_z^0 = |(\mathbf{B}, \mathbf{q}_2)|/B$ .

The parameter  $s$  is not continuous in our fundamental domain and has singularities on the levels of  $p_z$ , containing singular points within the domain. As we will see, this circumstance will not actually be important in our considerations. Let us put that the values of  $s$  are restricted by the values  $s_1(p_z)$  and  $s_2(p_z)$  at a given value of  $p_z$  for our fundamental domain. The functions  $s_1(p_z)$  and  $s_2(p_z)$  also have singularities at the same  $p_z$ , defined by the singular behavior of  $s_2(p_z) - s_1(p_z)$ :

$$s_2(p_z) - s_1(p_z) \sim |\ln(|\Delta p_z|/p_z^0)|$$

near the singular levels.

It's not difficult to see also that the singularities of  $s_2(p_z) - s_1(p_z)$  have asymmetric character since the corresponding trajectories approach the singular point once or twice depending on the sign of  $\Delta p_z$ . Let us note here that the last circumstance played important role in the proof of the fact of mixing in the dynamical systems analogous to those considered here. This property was proved

in paper [31] where systems of this kind were considered in connection with a different problem of Hamiltonian dynamics ([2]).

Every trajectory with the period  $\mathbf{q} = k_1\mathbf{q}_1 + k_2\mathbf{q}_2$  is represented in our domain by  $|k_1| + |k_2|$  separate lines, giving a closed curve after the identification of the equivalent points in the  $\mathbf{p}$ -space. The values of the functions  $\langle v_{gr}^l \rangle_{tr}$  are the same on every set of  $|k_1| + |k_2|$  components representing one periodic trajectory.

The presence of singular points plays also important role in the global motion of electrons along the non-singular trajectories since they appear many times at rather small distances from a periodic trajectory with a large period  $\mathbf{q} = k_1\mathbf{q}_1 + k_2\mathbf{q}_2$ . As a result, the length  $S$  of a periodic trajectory in the parameter  $s$  ( $S \sim |k_1| + |k_2|$ ) has essential fluctuations, caused by the presence of singular points in the fundamental domain. Let us note, that according to system (I.1) we can write in our coordinate system

$$\langle v_{gr}^l \rangle_{tr} = L(k_1, k_2) / S(p_z) , \quad (\text{III.14})$$

where  $L(k_1, k_2)$  is the length of the corresponding topological cycle in the  $\mathbf{p}$ -space, depending just on the numbers  $(k_1, k_2)$ . In general, we have  $(|k_1| + |k_2|) \cdot N$  singular points  $p_z^j \in [0, p_z^0]$  of the function  $S(p_z)$ , where  $N$  is the number of (non-equivalent) singular points of system (I.1) on the carrier of open trajectories.

The function  $S(p_z)$  represents a periodic function with the period  $P = p_z^0 / (|k_1| + |k_2|)$  and integrable (asymmetric) singularities

$$S(p_z) \sim \ln(p_z^0 / |\Delta p_z|)$$

at the values of  $p_z$  corresponding to singular electron trajectories. In particular, in the interval  $I^j = [p_z^j, p_z^{j+1}]$ , restricted by two subsequent "singular" values of  $p_z$  ( $|p_z^{j+1} - p_z^j| \leq P$ ), we can write the contribution of the singularities at the points  $p_z^j$  and  $p_z^{j+1}$  to the value of  $S(p_z)$  in the form

$$\delta_1 S(p_z) \sim \alpha_+^j \ln(p_z^0 / (p_z - p_z^j)) + \alpha_-^{j+1} \ln(p_z^0 / (p_z^{j+1} - p_z)) , \quad (\text{III.15})$$

( $\alpha_+^j, \alpha_-^{j+1} \sim 1$ ).

Besides that, the singularities at the points  $(\dots, p_z^{j-2}, p_z^{j-1})$  and  $(p_z^{j+2}, \dots)$ , close to the interval  $I^j$ , play also in fact important role for the variations of  $S(p_z)$  inside the interval  $I^j$  for big values of  $k_1$  and  $k_2$ .

The corresponding contribution to  $S(p_z)$  can be written as a sum of terms analogous to (III.15), which number is proportional to  $|k_1| + |k_2|$ . We actually will be interested here in the fluctuations of  $S(p_z)$  caused by these singularities, so only the variation of this contribution with the variable  $p_z$  is important for us. It's not difficult to show also that the difference of this contribution at the points  $p_z^j$  and  $p_z^{j+1}$  has the order  $\sim \ln(|k_1| + |k_2|)$ . For



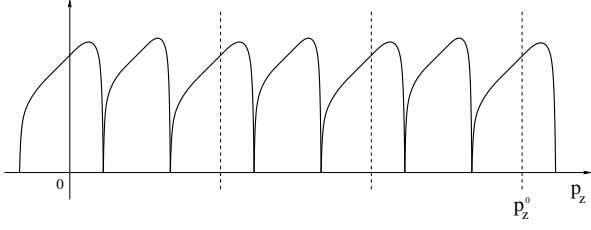


FIG. 21: The general form of the periodic function  $\langle v_{gr}^y \rangle_{tr}(p_z)$  on a carrier of open trajectories for the case of rational mean direction  $\mathbf{q} = k_1\mathbf{q}_1 + k_2\mathbf{q}_2$  of the trajectories.

our purposes here (we omit here rigorous estimations) the corresponding contribution  $\delta_2 S(p_z)$  to the function  $S(p_z)$  can be actually approximated by a linear function

$$\delta_2 S(p_z) \sim \Gamma^j (|k_1| + |k_2|) \ln(|k_1| + |k_2|) \frac{p_z - p_z^j}{p_z^0},$$

( $|\Gamma^j| \sim 1$ ), on every interval  $I^j$ .

The functions  $\delta_1 S(p_z)$  and  $\delta_2 S(p_z)$  represent the main corrections to the “basic value”  $\bar{S}$  of the function  $S(p_z)$ , which are responsible for the main terms in the dependence of  $\Delta\sigma_\infty^{kl}(\mathbf{B}/B) - \Delta\bar{\sigma}_\infty^{kl}(\mathbf{B}/B)$  on the numbers  $(k_1, k_2)$  (or  $(m_1, m_2, m_3)$ ). The basic value  $\bar{S}$  of the function  $S(p_z)$  is given by a constant function on the whole interval  $[0, p_z^0]$ , which in the main order is proportional to the length  $L(k_1, k_2)$  (or  $L(m_1, m_2, m_3)$ ) of the topological cycle  $(m_1, m_2, m_3)$  in the  $\mathbf{p}$ -space. Easy to see that for any sequence of rational directions converging to some fixed (irrational) direction we can write in the main order  $L(k_1, k_2) \sim |k_1| + |k_2|$ .

The functions  $\langle v_{gr}^y \rangle_{tr}$ ,  $\langle v_{gr}^z \rangle_{tr}$  are continuous functions of  $p_z$ , however, they are not smooth on the curves, representing singular trajectories. Thus, for the component  $v_{gr}^y$  we can write the following relations

$$\langle v_{gr}^y \rangle_{tr} \sim [\ln(p_z^0/|\Delta p_z|)]^{-1} \rightarrow 0$$

near these curves. In general, the values  $\langle v_{gr}^y \rangle_{tr}$  represent a periodic function of  $p_z$  with the period  $P = p_z^0/(|k_1| + |k_2|)$  and very narrow cusps at the values of  $p_z$ , corresponding to singular electron trajectories (Fig. 21). It is easy to see also that the number of cusps on the period of the function  $\langle v_{gr}^y \rangle_{tr}$  is equal to the number  $N$  of non-equivalent singular points of system (I.1) on the corresponding carrier of open trajectories.

In our situation we can put approximately

$$\begin{aligned} S(p_z) &\simeq \bar{S} + \delta_1 S(p_z) + \delta_2 S(p_z) \sim \\ &\sim |k_1| + |k_2| + \alpha_+^j \ln(p_z^0/(p_z - p_z^j)) + \\ &\quad + \alpha_-^{j+1} \ln(p_z^0/(p_z^{j+1} - p_z)) + \\ &\quad + \Gamma^j (|k_1| + |k_2|) \ln(|k_1| + |k_2|) \frac{p_z - p_z^j}{p_z^0}, \end{aligned}$$

and

$$\langle v_{gr}^y \rangle_{tr} \simeq L(k_1, k_2) / (\bar{S} + \delta_1 S(p_z) + \delta_2 S(p_z))$$

on every interval  $I^j$ . Let us say that the approximation above should be used in our scheme also for the calculation of the approximate values of  $\langle v_{gr}^y \rangle_{\hat{S}_F^\gamma}$  according to formula (III.13). Using this approximation to compute the values

$$\begin{aligned} \Delta\sigma_\infty^{kl}(\mathbf{B}/B) - \Delta\bar{\sigma}_\infty^{kl}(\mathbf{B}/B) &= \\ &= e^2 \tau \sum_\gamma \iint_{\hat{S}_F^\gamma} \langle v_{gr}^k \rangle_{tr} \langle v_{gr}^l \rangle_{tr} \frac{dp_z ds}{(2\pi\hbar)^3} - \\ &- e^2 \tau \sum_\gamma \iint_{\hat{S}_F^\gamma} \langle v_{gr}^k \rangle_{\hat{S}_F^\gamma} \langle v_{gr}^l \rangle_{\hat{S}_F^\gamma} \frac{dp_z ds}{(2\pi\hbar)^3} \end{aligned} \quad (\text{III.16})$$

for  $k, l = 2$ , we finally get the relations

$$|\Delta\sigma_\infty^{22}(\mathbf{B}/B) - \Delta\bar{\sigma}_\infty^{22}(\mathbf{B}/B)| \sim \frac{\ln^2(|k_1| + |k_2|)}{(|k_1| + |k_2|)^2}$$

To give the necessary approximation for the function  $\langle v_{gr}^z \rangle_{tr}$  we have to evaluate also the integral

$$J(p_z) = \oint v_{gr}^z(p_z, s) ds$$

over a periodic trajectory.

First, we should note, that we have to prescribe here also the “basic value”

$$J(p_z) \simeq \bar{J} \simeq \bar{v}_{gr}^z (|k_1| + |k_2|)$$

to this integral, which is constant on the interval  $[0, p_z^0]$ . The essential corrections to the value  $\bar{J}$  on the intervals  $I^j$  are caused again by the presence of singular points and can be represented by two main contributions:

1) The contribution of the endpoints of  $I^j$ , which can be approximately written as

$$\begin{aligned} \delta_1 J(p_z) &\simeq v_j^z \alpha_+^j \ln(p_z^0/(p_z - p_z^j)) + \\ &\quad + v_{j+1}^z \alpha_-^{j+1} \ln(p_z^0/(p_z^{j+1} - p_z)), \end{aligned}$$

where  $v_j^z$  and  $v_{j+1}^z$  are the values of  $v_{gr}^z$  at the singular points, adjacent to the corresponding singular trajectories;

2) The contribution of other singular points close to the interval  $I^j$ , which can again be approximated by the linear function

$$\delta_2 J(p_z) \simeq v_*^z \Gamma^j (|k_1| + |k_2|) \ln(|k_1| + |k_2|) \frac{p_z - p_z^j}{p_z^0},$$

where  $v_*^z$  represents some weighted average of the values  $v_j^z$  over all the singular points in the fundamental domain.

We can use now the following approximation for the function  $\langle v_{gr}^z \rangle_{tr}(p_z)$ :

$$\begin{aligned} \langle v_{gr}^z \rangle_{tr}(p_z) &\simeq \\ &\simeq (\bar{J} + \delta_1 J(p_z) + \delta_2 J(p_z)) / (\bar{S} + \delta_1 S(p_z) + \delta_2 S(p_z)) \end{aligned} \quad (\text{III.17})$$

We can see here that the function  $\langle v_{gr}^z \rangle_{tr}(p_z)$  does not have cusps at the values  $p_z^j$  and the values  $\langle v_{gr}^z \rangle_{tr}(p_z^j)$  are equal to  $v_z^j$ . However, the structure of the function  $\langle v_{gr}^z \rangle_{tr}(p_z)$  still has many common features with the structure of the function  $\langle v_{gr}^y \rangle_{tr}(p_z^j)$ . In particular, using the approximation (III.17) in the formula (III.16), we obtain actually the same relations

$$|\Delta \sigma_\infty^{kl}(\mathbf{B}/B) - \Delta \bar{\sigma}_\infty^{kl}(\mathbf{B}/B)| \sim \frac{\ln^2(|k_1| + |k_2|)}{(|k_1| + |k_2|)^2} \quad (\text{III.18})$$

for  $k, l = 2, 3$ , which implies also relations (II.2) for a given Stability Zone  $\Omega_\alpha$ .

The arguments used above can be applied also to the estimation of the functions  $q(B)$ ,  $r(B)$ ,  $p(B)$  in relations (II.7). Let us say at once, that we will not present here rigorous calculations, however, the approximate considerations below capture all the essential features which are necessary for our purposes. Thus, for the estimation of the functions (III.9) we can use the approximation when the integration in (III.9) is taken just over a part of a trajectory having length  $\sim eB\tau/c$  in the parameter  $s$ . In the same way, we can use for the averaged values

$$\langle v_{gr}^k \rangle_B(p_z, s) \equiv \frac{c}{eB\tau} \int_{-\infty}^s v_{gr}^k(p_z, s') e^{\frac{c(s'-s)}{eB\tau}} ds' \quad (\text{III.19})$$

the approximation

$$\langle v_{gr}^k \rangle_B(p_z, s) \simeq \frac{c}{eB\tau} \int_{s-eB\tau/c}^s v_{gr}^k(p_z, s') ds'$$

Let us take again the fundamental domain in the form shown at Fig. 20. The open trajectories have now irrational mean direction and are not periodic in the  $\mathbf{p}$ -space anymore. The corresponding parts of open trajectories are represented by nets of approximately  $eB\tau/m^*c = \omega_B\tau$  curves in the fundamental domain with approximate distances  $\sim p_z^0/\omega_B\tau$  between the curves.

The functions  $\langle v_{gr}^k \rangle_B(p_z, s)$  are almost constant along the curves  $p_z = \text{const}$  in the fundamental domain and change for the most part along the coordinate  $p_z$ . For generic mean direction of open trajectories the functions  $\langle v_{gr}^{2,3} \rangle_B(p_z, s)$  do not have periods smaller than  $p_z^0$  in the fundamental domain, however, in other essential features the behavior of  $\langle v_{gr}^{2,3} \rangle_B(p_z, s)$  in our approximation is similar to the above behavior of the functions  $\langle v_{gr}^{2,3} \rangle_{tr}(p_z)$ , considered for a rational mean direction of open trajectories with  $|k_1| + |k_2| \simeq \omega_B\tau$ . In particular,

we can also introduce here the values  $p_z^j$  in the fundamental domain, defined by the requirement of presence of a singular point on the preceding part of the corresponding trajectory at a distance not exceeding the value  $\sim \omega_B\tau p_F$  in the  $\mathbf{p}$ -space. The number of the values  $p_z^j$  in the fundamental domain has the order  $\sim \omega_B\tau$  for  $B \rightarrow \infty$  and we can consider again the division of the interval  $[0, p_z^0]$  to the segments  $I^j$  analogous to those considered above. The similar analysis shows also that the behavior of the functions  $\langle v_{gr}^{2,3} \rangle_B(p_z, s)$  demonstrates on the intervals  $I^j$  the features analogous to those observed in the behavior of  $\langle v_{gr}^{2,3} \rangle_{tr}(p_z)$  for a rational mean direction of the open trajectories with the numbers  $k_1, k_2$  having the order  $\omega_B\tau$ .

Let us introduce now the symmetric and the anti-symmetric parts of the conductivity tensor

$$\sigma^{kl} = s^{kl} + a^{kl}$$

According to the Onsager relations we have the identities

$$s^{kl}(-\mathbf{B}) = s^{kl}(\mathbf{B}) \quad a^{kl}(-\mathbf{B}) = -a^{kl}(\mathbf{B})$$

After some elementary calculations we can get from the formula (III.11):

$$\Delta s^{kl}(B) = e^2 \tau \sum_\gamma \iint_{\hat{S}_F^\gamma} \langle v_{gr}^k \rangle_B \langle v_{gr}^l \rangle_B \frac{dp_z ds}{(2\pi\hbar)^3}, \quad (\text{III.20})$$

$$\begin{aligned} \Delta a^{kl}(B) &= \\ &= \frac{e^2 \tau}{2} \sum_\gamma \iint_{\hat{S}_F^\gamma} \left( v_{gr}^k \langle v_{gr}^l \rangle_B - \langle v_{gr}^k \rangle_B v_{gr}^l \right) \frac{dp_z ds}{(2\pi\hbar)^3} \end{aligned} \quad (\text{III.21})$$

It is not difficult to see that for any irrational mean direction of the open trajectories the values  $\langle v_{gr}^k \rangle_B, \langle v_{gr}^l \rangle_B$  coincide with the values  $\langle v_{gr}^k \rangle_{\hat{S}_F^\gamma}, \langle v_{gr}^l \rangle_{\hat{S}_F^\gamma}$  in the limit  $B \rightarrow \infty$ . At the same time, for large but finite values of  $B$  the behavior of the functions  $\langle v_{gr}^{2,3} \rangle_B(p_z, s)$  is analogous to the behavior of  $\langle v_{gr}^{2,3} \rangle_{tr}$  for a rational mean direction of the open trajectories with  $k_1, k_2 \simeq \omega_B\tau$ . As a result, in full analogy with formula (III.16), we can write the relations

$$\Delta s^{kl}(B) - \Delta s_\infty^{kl} \simeq \frac{\ln^2(\omega_B\tau)}{(\omega_B\tau)^2}, \quad k, l = 2, 3 \quad (\text{III.22})$$

for generic directions of the open trajectories.

It is easy to see that the estimation (III.22) gives now the relations (II.9) for the functions  $q(B)$  and  $p(B)$ . At the same time, the relations (II.10) for the function  $r(B)$  are defined by the behavior of the anti-symmetric part of the tensor  $\sigma^{kl}(B)$ . Using the same approximations for the functions  $\langle v_{gr}^{2,3} \rangle_B(p_z, s)$ , we get now the estimation

$$|\Delta a^{23}(B)| \leq \frac{\ln \omega_B\tau}{\omega_B\tau}, \quad (\text{III.23})$$

Using also the identity  $a_\infty^{kl} \equiv 0$  we then get relations (II.10) for the function  $r(B)$ .

Let us say that a unified description of the function  $\Delta a^{23}(B)$  can not be actually obtained in general situation, since its the behavior admits really essential variations depending on a concrete form of the Fermi surface.

As we said already, the relations (III.22) can be considered just as a “general trend” in the behavior of conductivity in strong magnetic fields. Let us give here a more detailed explanation of our statement.

As we can see, the analogy between the relations (III.18) and (III.22) requires in fact the assumption of the “uniform covering” of the carrier of open trajectories by parts of the trajectories having length  $\simeq \omega_B \tau p_F$ . This assumption is fulfilled “in average”, however, it can be violated for concrete values of  $\omega_B \tau$  for special directions of the open trajectories. It is not difficult to see, that this violation definitely takes place when the direction of the open trajectories can be approximated by a rational direction with a very high precision ( $\ll |k_1| + |k_2|$ ). As we can see, the corresponding open trajectories will then be very close to the periodic trajectories on the lengths

$$\omega_B \tau p_F \gg (|k_1| + |k_2|) p_F ,$$

so the parameter  $|k_1| + |k_2|$  should be actually used instead of  $\omega_B \tau$  in (III.22) up to the values  $\omega_B \tau \gg |k_1| + |k_2|$ . As a result, the general trend (III.22) can have essential corrections.

For better description of the behavior of  $\sigma^{kl}(B)$  for generic mean directions of the stable open trajectories let us just say some words about the problem of approximation of irrational numbers by rational ones. In our case we have to investigate the possibility of rational approximations of the number  $\kappa$  in relation (II.6), which correspond to rational approximations of the mean direction of the open trajectories in the plane  $\Gamma_\alpha$ .

According to classical (Dirichlet) theorem we can state that for any number  $N \in \mathbb{N}$  there exist two integer numbers  $k_1, k_2$ :

$$1 \leq k_1 \leq N \quad , \quad k_1, k_2 \in \mathbb{Z} \quad ,$$

such that

$$\left| \kappa - \frac{k_2}{k_1} \right| < \frac{1}{k_1 N} \quad (III.24)$$

Let us note here that we can put without loss of generality  $|\kappa| < 1$ , so we will assume also  $|k_2| \leq |k_1|$  for precise approximations of  $\kappa$ .

For the value  $N \simeq \omega_B \tau$  we can rewrite the relation (III.24) in the form

$$\omega_B \tau p_F \left| \kappa - \frac{k_2}{k_1} \right| < \frac{p_F}{k_1} \quad , \quad (III.25)$$

which means that the deviation of the open trajectory from the corresponding periodic trajectory does not exceed the value  $\simeq p_F/k_1$  on the length  $L \simeq \omega_B \tau p_F$ .

The relation (III.25) can be considered as the first step in the approximation of irrational directions of open trajectories by rational ones since the mean distance between the curves representing a periodic trajectory in the fundamental domain is of order of

$$p_F/(|k_1| + |k_2|) \simeq p_F/k_1 \quad .$$

We have to say, however, that relation (III.25) does not give a precise connection between the values  $\omega_B \tau$  and  $k_1$ , so this connection should be specially studied for every concrete irrational number  $\kappa$ . Using the theorem of Dirichlet, we can see that for any irrational number  $\kappa$  there always exists an infinite sequence of rational approximations

$$k_2^{(s)}/k_1^{(s)} \quad , \quad s = 1, \dots, \infty \quad ,$$

such that the following relations

$$\left| \kappa - \frac{k_2^{(s)}}{k_1^{(s)}} \right| < \frac{1}{(k_1^{(s)})^2} \quad (III.26)$$

take place for every  $s$ . If we consider now a sequence  $B^{(s)}$  of the values of  $B$ , such that  $\omega_{B^{(s)}} \tau \simeq k_1^{(s)}$ , we get the relations

$$\omega_{B^{(s)}} \tau p_F \left| \kappa - \frac{k_2^{(s)}}{k_1^{(s)}} \right| < \frac{p_F}{k_1^{(s)}} \quad ,$$

analogous to (III.25), for this sequence.

It can be seen, that the estimation above should not cause in general crucial deviations from the general trend according to our picture.

Let us say, however, that the estimation (III.26) can be actually improved if we consider “generic” irrational numbers  $\kappa$ , representing a set of the full measure in  $\mathbb{R}$ . For example, the following theorem can be formulated for generic  $\kappa$ :

Theorem (see e.g. [14]):

Let  $f(x)$  be a positive function of positive  $x$ , such that the function  $xf(x)$  is non-increasing. Then for almost all irrational  $\kappa$  the inequality

$$\left| \kappa - \frac{k_2^{(s)}}{k_1^{(s)}} \right| < \frac{f(k_1^{(s)})}{k_1^{(s)}}$$

has infinitely many solutions  $(k_1^{(s)}, k_2^{(s)})$  if for some positive  $c$  the integral

$$\int_c^\infty f(x) dx$$

is divergent.

The theorem above gives an improvement of the estimation (III.26) for “almost all” irrational numbers  $\kappa$  in the sense of the standard measure in  $\mathbb{R}$ . Easy to see, that the set of the functions  $f(x)$ , which can be used for

the improvement of the estimation (III.26), is rather big. For example, we can put

$$f_1(x) = [x \ln x]^{-1} \quad , \quad x > 1 \quad ,$$

$$f_2(x) = [x \ln x \ln \ln x]^{-1} \quad , \quad x > e \quad ,$$

etc. In particular, using the function  $f_1(x)$ , we get for the corresponding sequence of  $B^{(s)}$  the estimation

$$\omega_{B^{(s)}} \tau p_F \left| \kappa - \frac{k_2^{(s)}}{k_1^{(s)}} \right| < \frac{p_F}{k_1^{(s)} \ln k_1^{(s)}} \quad , \quad (\text{III.27})$$

( $\omega_{B^{(s)}} \tau \simeq k_1^{(s)}$ ).

The estimation above shows that the general trend (II.9) for the functions  $q(B)$ ,  $p(B)$  should have in fact an additional structure represented by the presence of “plateaus” near the values  $B^{(s)}$ .

As we said already, the estimation (III.27) can be used for “almost all” irrational numbers, characterizing the mean direction of open trajectories. For special irrational numbers these estimations can be much stronger and we should say in this case that the corresponding number has “very good” approximations by rational numbers.

As we can see then, the general trend in the behavior of  $s^{kl}(B)$  ( $k, l = 2, 3$ ) can be understood as an implementation of the relations (II.9) for the “reference values” of  $B$ , which represent an infinite sequence on the interval  $m^*c/e\tau < B < \infty$ . At the same time, near the values  $B^{(s)}$  the behavior of  $s^{kl}(B)$  demonstrates some kind of “plateaus” where the local dependence on  $B$  is actually different from the general trend. As a result, the global behavior of  $s^{kl}(B)$ ,  $k, l = 2, 3$  demonstrates a kind of “cascade structure” defined by the properties of the irrationality  $\kappa$ . Let us note also that the cascade structure is more distinct for the numbers  $\kappa$ , having better rational approximations, and is smoothed for generic irrational  $\kappa$ .

According to the above remark, we can also see that the trend (II.9) has in some sense “conventional” character and can be also considered just as a convenient choice among close possible descriptions of the asymptotic behavior of conductivity. We have to note also that in the special case when the carriers of open trajectories do not contain holes with singular points the relations (II.9) should be actually changed to the simpler trend

$$q(B) \sim p(B) \sim (\omega_B \tau)^{-1}$$

As it is not difficult to see, all the remarks above apply also to the estimation (III.23), which can be violated in the same situations as (III.22). For this reason, we should consider the relation (II.10) just as a “reliable” restriction on the function  $r(B)$ , defined by relation (II.7).

At the end of this section, let us consider the behavior of the components  $\sigma^{kl}(B)$ , where  $k$  or  $l$  is equal to 1. Let us note here that relations (II.7) represent in this

case the main terms in the behavior of these components which determines the difference between the functions  $a(B)$ ,  $b(B)$ ,  $c(B)$  and  $q(B)$ ,  $r(B)$ ,  $p(B)$ . According to system (I.1) the integral

$$\int_{-\infty}^s v_{gr}^x(p_z, s') ds'$$

represents the value  $-p_y(s) + \text{const}$  and is a bounded function in our coordinate system. An elementary estimation of the integral (III.19) gives now the main term

$$\langle v_{gr}^1 \rangle_B(p_z, s) \sim (\omega_B \tau)^{-1} \quad (\text{III.28})$$

in the asymptotic behavior of the function  $\langle v_{gr}^1 \rangle_B$ , which can be used in the formulae (III.20) - (III.21). In particular, we easily get from (III.20) the relation

$$\Delta \sigma^{11}(B) \sim (\omega_B \tau)^{-2} \quad ,$$

which, being added also with the corresponding term of (I.6), gives the first part of the relation (II.8).

Let us note now that the value  $\langle v_{gr}^1 \rangle_B$  demonstrates also the property

$$\iint_{\hat{S}_F^\gamma} \langle v_{gr}^1 \rangle_B(p_z, s) \frac{dp_z ds}{(2\pi\hbar)^3} = 0$$

(view the same property of  $v_{gr}^1(p_z, s)$ ). Using the representation

$$\langle v_{gr}^l \rangle_B = \langle v_{gr}^l \rangle_{\hat{S}_F^\gamma} + o(1) \quad , \quad B \rightarrow \infty$$

( $l = 2, 3$ ) for generic mean direction of the open trajectories in the formula (III.20), we then get the relations

$$\Delta s^{12}(B) \sim \Delta s^{13}(B) = o((\omega_B \tau)^{-1})$$

for the symmetric part of  $\Delta \sigma^{kl}(B)$ .

We can see then, that the main terms in the asymptotic behavior of the values  $\sigma^{ll}(B)$ ,  $\sigma^{k1}(B)$ , ( $l, k = 2, 3$ ) are defined by the anti-symmetric part of the conductivity tensor. To estimate the corresponding terms let us note now that the estimation (III.28) is also valid for the function

$$\langle v_{gr}^1 \rangle_{-B}(p_z, s) \equiv \frac{c}{eB\tau} \int_s^{+\infty} v_{gr}^1(p_z, s') e^{\frac{c(s-s')}{eB\tau}} ds'$$

for our type of open trajectories. Using now the change of the order of integration in formula (III.21) we can write

$$\begin{aligned} \Delta a^{1l}(B) &= \\ &= \frac{e^2 \tau}{2} \sum_\gamma \iint_{\hat{S}_F^\gamma} \left( \langle v_{gr}^1 \rangle_{-B} - \langle v_{gr}^1 \rangle_B \right) v_{gr}^l \frac{dp_z ds}{(2\pi\hbar)^3} \end{aligned}$$

( $l = 2, 3$ ), which gives the necessary estimation for the functions  $\Delta a^{ll}(B)$ . Adding also the anti-symmetric part

of the tensor (I.6), we get finally the remaining part of the relation (II.8).

Let us note also that the higher corrections to the components  $\sigma^{ll}(B)$ ,  $\sigma^{kl}(B)$  have more complicated behavior for generic open trajectories in  $\mathbf{p}$ -space but usually are not considered in applications.

Let us say here, that the structure of  $\sigma^{kl}(B)$  described above has in some sense abstract theoretical character and probably can not be observed in all features in most of the experiments. However, we expect that the basic elements of the picture described above still can be detected in special studies of the conductivity behavior in strong magnetic fields. In general, we can expect that in the most of the real experiments it can be just established that the values  $\sigma^{kl}(B) - \bar{\sigma}_{\infty}^{kl}$ ,  $k, l = 2, 3$  demonstrate some general decreasing with the increasing of  $B$  with not uniquely specified decreasing law. Quite often it is convenient to approximate the behavior of  $\sigma^{kl}(B)$  by some intermediate powers  $(\omega_B \tau)^\mu$  of the parameter  $\omega_B \tau$ , however, we should admit an irregular dependence of the parameter  $\mu$  on the direction and the value of  $\mathbf{B}$  in this case. Let us say also that the right-hand parts in (III.22) - (III.23) can arise with big dimensionless coefficients having geometric origin, so for complicated Fermi surfaces the interplay between the values  $\bar{\sigma}_{\infty}^{kl}$  and  $q^2(B)$ ,  $r(B)$ ,  $p^2(B)$  can be important even for rather big values of  $\omega_B \tau$ .

Let us say that the questions considered above are connected mostly with the geometry of the stable open trajectories. In the next section we will consider the aspects of the conductivity behavior connected with the reconstruction of the trajectories of this type.

#### IV. THE RECONSTRUCTION OF THE OPEN TRAJECTORIES AND THE CONDUCTIVITY BEHAVIOR IN THE “EXPERIMENTALLY OBSERVABLE STABILITY ZONE” $\Omega_{\alpha}$ .

To explain the behavior of conductivity in the Zone  $\Lambda_{\alpha}$  we have to consider the reconstruction of the carriers of open trajectories after crossing the boundary of the Zone  $\Omega_{\alpha}$  on the unit sphere. In general, the most essential features of such reconstruction can be demonstrated by the following simplified scheme:

Let us imagine the Fermi surface in  $\mathbb{R}^3$  in the form of an infinite set of integral planes (with holes) connected by parallel cylinders of finite heights (Fig. 22). It is assumed that all the planes are divided into the “even-numbered” and the “odd-numbered” planes, which gives also the separation of the cylinders into two different classes. We will assume here, that all the planes of a given class represent the same object after the factorization over the reciprocal lattice vectors and the same is assumed also about the cylinders of a given class. Thus, the physical Fermi surface represents here two parallel two-dimensional tori (with holes)  $\mathbb{T}^2 \subset \mathbb{T}^3$  connected by two cylinders in  $\mathbb{T}^3$ .

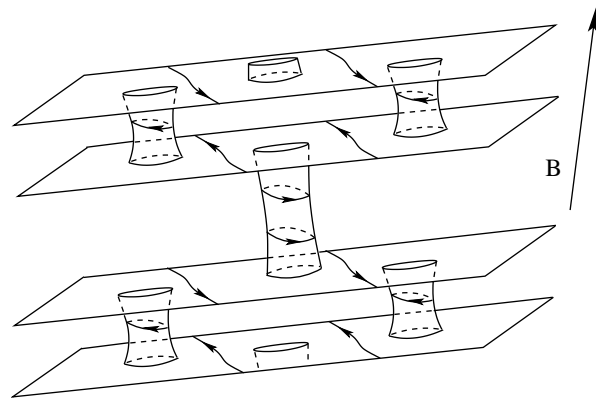


FIG. 22: The simplified (schematic) Fermi surface, used for demonstration of the main features arising at the boundary of the Stability Zone  $\Omega_{\alpha}$ .

It is easy to see that for those  $\mathbf{B}$ , which are almost parallel to the axes of the cylinders, the cylinders constructed above represent cylinders of closed electron trajectories, while the planes with holes play the role of carriers of open trajectories. It can be seen also, that the open trajectories on the planes of different types represent the motion in two opposite directions, while two types of finite-sized cylinders carry closed trajectories of the “electron type” and the “hole type” respectively. Thus, we get a Stability Zone  $\Omega_{\alpha}$  around the direction  $\hat{\mathbf{B}}^{\parallel}$ , parallel to the axes of the cylinders connecting the integral planes.

The cylinders of the closed trajectories almost coincide with the cylinders, connecting the planes, for directions of  $\mathbf{B}$ , close to  $\hat{\mathbf{B}}^{\parallel}$ , however, they become shorter and represent just parts of these cylinders for  $\mathbf{B}$ , deviating from the direction  $\hat{\mathbf{B}}^{\parallel}$ . The boundary of the Zone  $\Omega_{\alpha}$  is defined by the condition that the height of the cylinders of closed trajectories of one type (say, electron type) becomes zero, while the height of the cylinders of closed trajectories of another type remains finite. After crossing the boundary of  $\Omega_{\alpha}$  the individual integral planes do not represent carriers of open trajectories anymore, however, we can still claim that near the boundary of  $\Omega_{\alpha}$  the cylinders of closed trajectories of the second type cut our Fermi surface into pairs of connected integral planes in  $\mathbb{R}^3$ . So, we can investigate here the behavior of trajectories of system (I.1) separately on these separated parts of the Fermi surface, which gives actually rather simple description of the trajectories in  $\mathbb{R}^3$ :

Let us denote here by  $\Gamma_{\alpha}$  the integral plane, giving the common integral direction of the planes considered above, and by  $\Pi(\mathbf{B})$  the plane orthogonal to  $\mathbf{B}$ . It is not difficult to see that in the picture described above all the trajectories on our Fermi surface become closed if the intersection of  $\Gamma_{\alpha}$  and  $\Pi(\mathbf{B})$  has irrational direction.

The appearance of the closed trajectories on every pair of connected planes can be considered as a result of a re-

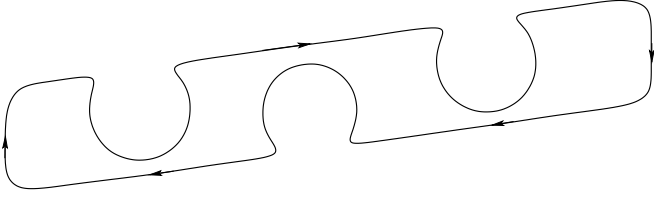


FIG. 23: The long closed trajectories arising as a result of a reconstruction of a pair of open trajectories on a pair of connected planes after crossing the boundary of the Zone  $\Omega_\alpha$  on the angle diagram.

construction of the open trajectories, which is caused by the “jumps” of the trajectories between two planes outside  $\Omega_\alpha$  (Fig. 23). It is easy to see that these closed trajectories will have very big length in the immediate vicinity of the boundary of  $\Omega_\alpha$  due to the low probability of the “jumps” in this region. At the same time, it can be seen also that for any fixed irrational direction of intersection of  $\Gamma_\alpha$  and  $\Pi(\mathbf{B})$  all the open trajectories will necessarily pass through the reconstruction after the crossing the boundary of  $\Omega_\alpha$ .

The situation is rather different when the intersection of  $\Gamma_\alpha$  and  $\Pi(\mathbf{B})$  has a rational direction  $\mathbf{a}$ . In this case just a part of open trajectories undergoes reconstruction after the crossing the boundary of  $\Omega_\alpha$  by the direction of the magnetic field, while the other trajectories still remain open. So, in this situation the long and the open periodic trajectories coexist on the integral planes, having different measure for different directions of  $\mathbf{B}$ . It is not difficult to see also, that the open trajectories have the maximal measure near the boundary of  $\Omega_\alpha$  and disappear at the endpoints of the curve  $\hat{\gamma}_\mathbf{a}^\alpha$ .

From a simple estimation of the integrals in (III.10) we easily get that in the interval  $1 \ll \omega_B\tau \ll \lambda(\mathbf{B}/B)$  the contribution of the long closed trajectories to the conductivity is similar to that of the stable open trajectories, so we get formula (II.11) in this interval.

To estimate the contribution of the trajectories shown at Fig. 23 in the limit  $\omega_B\tau \gg \lambda(\mathbf{B}/B)$  let us just first note that we have in general the relations

$$\langle v_{gr}^y \rangle_{tr}(p_z) = 0 \quad , \quad \langle v_{gr}^z \rangle_{tr}(p_z) \neq 0$$

for this type of trajectories. At the same time, we can see that the trajectory shown at Fig. 23 can be considered as consisting of two parts belonging to different former carriers of open trajectories with opposite values of  $\langle v_{gr}^y \rangle_{\hat{S}_F^\gamma}$  and  $\langle v_{gr}^z \rangle_{\hat{S}_F^\gamma}$ . As a result, the typical value of  $\langle v_{gr}^z \rangle_{tr}$  on the closed trajectories is rather small and is defined by the density of the trajectory on the (former) carriers in the Brillouin zone. The exact dependence of  $\langle v_{gr}^z \rangle_{tr}(p_z)$  on the value  $\lambda(\mathbf{B}/B)$  can have in fact a complicated character, it's not difficult to see, however, that for our pretty rough definition of the function  $\lambda(\mathbf{B}/B)$  the simple approximation

$$\langle v_{gr}^z \rangle_{tr}(p_z) \sim \lambda^{-1}(\mathbf{B}/B)$$

can be used. It can be seen also that with the same accuracy we can also use the approximations

$$\langle v_{gr}^y \rangle_B \sim \langle v_{gr}^z \rangle_B - \langle v_{gr}^z \rangle_{tr} \sim \lambda(\mathbf{B}/B) / \omega_B\tau \quad (IV.1)$$

for large but finite values of  $B$ . At the same time, for the values  $\langle v_{gr}^x \rangle_B$  we can use the relation

$$\langle v_{gr}^x \rangle_B \sim \langle v_{gr}^x \rangle_{-B} \sim (\omega_B\tau)^{-1} \quad (IV.2)$$

for all  $\omega_B\tau \gg 1$ . Using the above relations, we then easily get from (III.20) the following estimations

$$\Delta s^{kl}(B) \simeq \frac{ne^2\tau}{m^*} \begin{pmatrix} 0 & 0 & 0 \\ 0 & 0 & 0 \\ 0 & 0 & * \cdot \lambda^{-2} \end{pmatrix} + \frac{ne^2\tau}{m^*} \begin{pmatrix} (\omega_B\tau)^{-2} & \lambda(\omega_B\tau)^{-2} & \lambda(\omega_B\tau)^{-2} \\ \lambda(\omega_B\tau)^{-2} & \lambda^2(\omega_B\tau)^{-2} & \lambda^2(\omega_B\tau)^{-2} \\ \lambda(\omega_B\tau)^{-2} & \lambda^2(\omega_B\tau)^{-2} & \lambda^2(\omega_B\tau)^{-2} \end{pmatrix}$$

for the contribution of the long closed trajectories to the symmetric part of the conductivity tensor. Let us note also here that the integration over a set of carriers of open trajectories  $\hat{S}_F = \cup \hat{S}_F^\gamma$  in formula (III.20) should be understood now as the integration over the part of the Fermi surface  $S_{LCT}$  occupied by the long closed trajectories.

Let us remind now, that the tensor  $\Delta s^{kl}(B)$  should be added also with the symmetric part of the contribution of the short closed trajectories extracted from the relations (I.6). As a result, the value  $s^{33}(B)$  will get in fact a finite contribution, which does not depend on the value of  $\lambda(\mathbf{B}/B)$ . We can claim, however, that the conductivity behavior demonstrates here a partial suppression of the conductivity along the direction of  $\mathbf{B}$ , which is expressed by the formula (II.13).

To evaluate the contribution of the long closed trajectories to the anti-symmetric part of the conductivity tensor we need actually a more detailed consideration of the behavior of  $v_{gr}^k(p_z, s)$  on the trajectories of this type. Thus, using formula (III.21) in the form

$$\begin{aligned} \Delta a^{kl}(B) &= \\ &= \frac{e^2\tau}{2} \iint_{S_{LCT}} \left( \langle v_{gr}^k \rangle_{-B} - \langle v_{gr}^k \rangle_B \right) v_{gr}^l \frac{dp_z ds}{(2\pi\hbar)^3} \quad , \end{aligned} \quad (IV.3)$$

we can easily get the estimation

$$\Delta a^{12}(B) \sim \Delta a^{13}(B) \sim (\omega_B\tau)^{-1}$$

from the relation (IV.2).

At the same time, the estimation of the value  $\Delta a^{23}(B)$  requires in fact a more detailed analysis of the formula (IV.3). Thus, the estimations (IV.1) can not be simply used in formula (IV.3) to get the corresponding estimation of  $\Delta a^{23}(B)$  because of the specific form of the trajectories shown at Fig. 23. Indeed, as can be easily seen,

the values  $v_{gr}^y(s)$  and  $v_{gr}^z(s)$  on the trajectories of this form are strongly correlated on big scales ( $\sim \lambda(\mathbf{B}/B)$ ), so, their slow harmonics will in fact annihilate each other in the anti-symmetric part of  $\sigma^{kl}(B)$ . More precisely, let us represent the values  $v_{gr}^k(p_z, s)$  on the long closed trajectories in the form

$$v_{gr}^k(p_z, s) = \sum_{m=-\infty}^{+\infty} v_{gr(m)}^k(p_z) \exp(im\omega_0(p_z)s) ,$$

( $v_{gr(-m)}^k = \bar{v}_{gr(m)}^k$ ), where

$$\omega_0(p_z) \simeq (m^* \cdot \lambda(\mathbf{B}/B))^{-1} .$$

It is not difficult to check then by direct calculation that the contribution of the long closed trajectories to the anti-symmetric part of the conductivity tensor can be written as

$$\begin{aligned} \Delta a^{kl}(B) &= \frac{ec}{2B} \int \frac{dp_z}{(2\pi\hbar)^3} \times \\ &\times \sum_{m=-\infty}^{+\infty} \frac{2\pi im \left( v_{gr(m)}^k \bar{v}_{gr(m)}^l - \bar{v}_{gr(m)}^k v_{gr(m)}^l \right)}{(m\omega_0(p_z))^2 + (c/eB\tau)^2} \end{aligned} \quad (\text{IV.4})$$

where the integration over  $p_z$  is taken along the heights of the cylinders of long closed trajectories. Let us note here that the net height of all non-equivalent cylinders of the long closed trajectories has the order of  $p_F/\lambda(\mathbf{B}/B)$  while the density of the frequencies  $\omega_{(m)}(p_z) = m\omega_0(p_z)$  is proportional to  $\lambda(\mathbf{B}/B)$ .

The correlation of the functions  $v_{gr}^y(p_z, s)$  and  $v_{gr}^z(p_z, s)$  on the trajectory means now that the coefficients  $v_{gr(m)}^y(p_z)$  and  $v_{gr(m)}^z(p_z)$  are phase correlated, i.e. have almost the same complex phases at small values of  $m$ . In general, we can use the estimation

$$\left| \text{Arg } v_{gr(m)}^y(p_z) - \text{Arg } v_{gr(m)}^z(p_z) \right| \sim \frac{|m|}{\lambda(\mathbf{B}/B)}$$

in the interval

$$-\lambda(\mathbf{B}/B) \leq m \leq \lambda(\mathbf{B}/B) .$$

At the same time, we can write for the same values of  $m$  the relations

$$\left| v_{gr(m)}^y \right| \simeq \left| v_{gr(m)}^z \right| \sim \lambda^{-1/2}(\mathbf{B}/B)$$

for the trajectories of our type.

As a result, we can write approximately

$$\left| 2\pi im \left( v_{gr(m)}^y \bar{v}_{gr(m)}^z - \bar{v}_{gr(m)}^y v_{gr(m)}^z \right) \right| \sim \frac{m^2}{\lambda^2(\mathbf{B}/B)}$$

in the interval  $|m| \leq \lambda(\mathbf{B}/B)$ .

Using the above estimations in the formula (IV.4) we can get now the regular expansion for the value  $\Delta a^{23}(B)$  in the region  $\omega_B\tau \gg \lambda(\mathbf{B}/B)$ , having the form

$$\begin{aligned} \Delta a^{23}(B) &\simeq \\ &\simeq (\omega_B\tau)^{-1} \left( \Delta a_{(0)}^{23} + \sum_{k \geq 1} \Delta a_{(k)}^{23} \left( \frac{\omega_B\tau}{\lambda} \right)^{-2k} \right) \end{aligned}$$

where all  $\Delta a_{(k)}^{23}$  have the order of  $ne^2\tau/m^*$ . In particular, we can write in the main order

$$\Delta a^{23}(B) \simeq \frac{ne^2\tau}{m^*} (\omega_B\tau)^{-1}$$

Finally, we can write the estimation

$$\Delta a^{kl}(B) \simeq \frac{ne^2\tau}{m^*} \begin{pmatrix} 0 & (\omega_B\tau)^{-1} & (\omega_B\tau)^{-1} \\ (\omega_B\tau)^{-1} & 0 & (\omega_B\tau)^{-1} \\ (\omega_B\tau)^{-1} & (\omega_B\tau)^{-1} & 0 \end{pmatrix}$$

for the contribution of the long closed trajectories to the anti-symmetric part of the conductivity tensor.

Easy to see also that after the addition of the contribution of the short closed trajectories we get finally the formula (II.14) for the anti-symmetric part of the conductivity tensor.

For the values  $\omega_B\tau \simeq \lambda(\mathbf{B}/B)$  formula (III.10) gives some intermediate regimes between (II.11) and (II.12) - (II.14) which have in general some irregular form. We don't consider here these regimes in detail and just speak of the experimental approach to description of  $\sigma^{kl}(B)$  using intermediate powers of  $\omega_B\tau$ . As we have already said, the corresponding powers of  $\omega_B\tau$  have in this case just a local character and are not well defined as stable characteristics of the conductivity behavior.

The schematic Fermi surface considered above looks rather special from the general point of view. However, it demonstrates all the main points of the behavior of open trajectories near the boundary of the Stability Zone  $\Omega_\alpha$  which are important for us. In general, the schematic picture represented above can be enriched by additional cylinders of closed trajectories, connecting the integral planes or just having a point as a cylinder base (Fig. 24). Theoretically, we can also consider the situation when the connected parts of the Fermi surface joining integral planes represent compound structures consisting of several cylinders of closed trajectories (in fact, this situation is extremely unlikely for real Fermi surfaces). Still, the main feature of the reconstruction of the carriers of open trajectories after crossing the boundary of  $\Omega_\alpha$  for generic Fermi surface is given by the vanishing of the height of one particular cylinder of closed trajectories and the division of the Fermi surface into the pairs of integral planes, separated by other cylinders of closed trajectories. The most general picture of the division of the Fermi surface for  $\mathbf{B} \in \Omega_\alpha$  is given actually by the scheme containing more than two non-equivalent integral planes

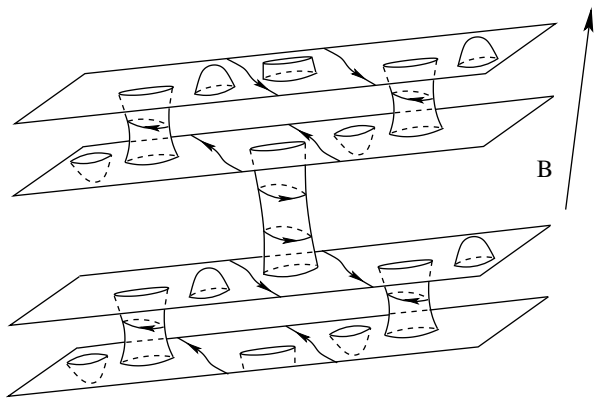


FIG. 24: More general schematic surface representing the structure of trajectories on real Fermi surface for directions of  $\mathbf{B}$  belonging to a fixed Stability Zone  $\Omega_\alpha$ .

(with the same integral direction), connected by cylinders of closed trajectories. In the last situation, which is theoretically possible for Fermi surfaces of very high genus, the pairs of integral planes and individual carriers of open trajectories can coexist after the reconstruction of a part of the open trajectories. Mathematically we will have in this case an overlapping of two Stability Zones  $\Omega_\alpha$  and  $\Omega'_\alpha$  with the same “topological quantum numbers”, which will result also in overlapping of the zones  $\hat{\Omega}_\alpha$  and  $\hat{\Omega}'_\alpha$  in the experimental study of conductivity. The full conductivity tensor in the overlappings

$$\Omega_\alpha \cap \Omega'_\alpha, \quad \Omega_\alpha \cap \Lambda'_\alpha, \quad \Lambda_\alpha \cap \Omega'_\alpha, \quad \Lambda_\alpha \cap \Lambda'_\alpha$$

is given in this case by the sum of the corresponding asymptotic expressions above, so we have here a theoretical possibility to observe very complicated analytical behavior of conductivity in the limit  $B \rightarrow \infty$ .

Let us point out here that the possibility of representation of the Fermi surface in the special form described above in the case of presence of stable open trajectories is based on rather deep topological theorems playing the most important role in the considerations of papers [8, 10, 36]. So, the picture described above represents in fact (under some generic requirements) the most general situation.

At the same time, we have to note that the statement above should be understood just as a topological characterization of system (I.1) in the case of presence of stable open trajectories. Thus, the topological structure shown at Fig. 24 can have in fact much more complicated (visual) geometric representation in the  $\mathbf{p}$ -space.

Finally, we can briefly describe the structure of the “experimentally observable Stability Zone”  $\hat{\Omega}_\alpha$ , arising in the quasiclassical approximation, as a union of the following main parts:

I) The central part of the Zone  $\hat{\Omega}_\alpha$  (containing the “mathematical Stability Zone”  $\Omega_\alpha$ ). The conductivity behavior in this part demonstrates the “most regular” de-

pendence on the value of  $B$ , represented by the asymptotic regimes (II.7) or (II.11). At the same time, the angular dependence of  $\sigma^{kl}(\mathbf{B})$  demonstrates here rather irregular character due to the presence of the “rational peaks” in the values of  $\sigma^{kl}(\mathbf{B})$  on a dense set of directions of  $\mathbf{B}$  in this area (Fig. 13).

II) The zone of rather complicated form around the central part of the Zone  $\hat{\Omega}_\alpha$  (the black area at Fig. 13). The tensor  $\sigma^{kl}(\mathbf{B})$  demonstrates here the most complicated dependence both on the value and the direction of  $\mathbf{B}$ , corresponding to a gradual transition from the regime (II.11) to (II.12) - (II.14). For an approximation of the behavior of  $\sigma^{kl}(\mathbf{B})$  the intermediate powers  $(\omega_B \tau)^\mu$  can be locally used, in general the value of  $\mu$  demonstrates unstable behavior. At the same time, the behavior of  $\sigma^{kl}(\mathbf{B})$  demonstrates a suppression of the conductivity along the direction of  $\mathbf{B}$  ( $\sigma^{33}(\mathbf{B})$ ) to some lower values on the exterior boundary of this zone.

III) The “boundary region” of the Zone  $\hat{\Omega}_\alpha$ . The behavior of  $\sigma^{kl}(\mathbf{B})$  demonstrates here a gradual transition from the regime (II.12) - (II.14) to the simpler behavior (I.4). The behavior of  $\sigma^{33}(\mathbf{B})$  demonstrates here a gradual increasing of the conductivity along the direction of  $\mathbf{B}$  to its maximal value on the boundary of  $\hat{\Omega}_\alpha$ .

At the end of the paper, we would like to make also one additional substantial remark. Namely, it can be actually shown, that the topological structure of system (I.1) admits also a similar description being considered for the whole dispersion relation  $\epsilon(\mathbf{p})$  and not just for a fixed Fermi level  $\epsilon = \epsilon_F$  (see [10]). In particular, the “Stability Zones” (corresponding to the presence of stable open trajectories at least at one energy level) can be introduced for the whole spectrum  $\epsilon(\mathbf{p})$ . From this point of view, the “experimentally observable Stability Zones”  $\hat{\Omega}_\alpha$  have in fact a connection with exact mathematical Stability Zones, defined for the whole energy spectrum. In particular, every “experimentally observable Stability Zone”  $\hat{\Omega}_\alpha$  always belongs to a bigger mathematical Stability Zone  $\Omega'_\alpha$ , defined for the whole spectrum  $\epsilon(\mathbf{p})$ .

## V. CONCLUSIONS.

We investigate the analytical behavior of conductivity of normal metals in strong magnetic fields in the case of presence of stable open electron trajectories on the Fermi surface. As it is shown in the paper, the behavior of conductivity can demonstrate rather nontrivial analytical properties in “experimentally observable Stability Zones” even under the condition  $\omega_B \tau \gg 1$ . In particular, in different parts of the experimentally observable Stability Zone the behavior of conductivity can demonstrate different types of “regular” or more complicated intermediate “irregular” regimes depending on the value of the magnetic field. The results of the paper are based on topological description of the carriers of open trajectories



on complicated Fermi surfaces obtained in recent mathematical investigations of the corresponding geometric

problem.

- 
- [1] A.A. Abrikosov., Fundamentals of the Theory of Metals., Elsevier Science & Technology, Oxford, United Kingdom, 1988.
- [2] V.I. Arnol'd., Topological and ergodic properties of closed 1-forms with incommensurable periods., *Functional Analysis and Its Appl.* **25**:2 (1991), 81-90.
- [3] R. De Leo., Existence and measure of ergodic leaves in Novikovs problem on the semiclassical motion of an electron., *Russian Math. Surveys* **55**:1 (2000), 166-168.
- [4] R. De Leo., Characterization of the set of "ergodic directions" in Novikov's problem of quasi-electron orbits in normal metals., *Russian Math. Surveys* **58**:5 (2003), 1042-1043.
- [5] R. De Leo., Topology of plane sections of periodic polyhedra with an application to the Truncated Octahedron., *Experimental Mathematics* **15**:1 (2006), 109-124.
- [6] R. De Leo, I.A. Dynnikov., An example of a fractal set of plane directions having chaotic intersections with a fixed 3-periodic surface., *Russian Math. Surveys* **62**:5 (2007), 990992.
- [7] R. De Leo, I.A. Dynnikov., Geometry of plane sections of the infinite regular skew polyhedron  $\{4, 6 | 4\}$ ., *Geom. Dedicata* **138**:1 (2009), 51-67.
- [8] I.A. Dynnikov., Proof S.P. Novikov's conjecture on the semiclassical motion of an electron., *Math. Notes* **53**:5 (1993), 495-501.
- [9] I.A. Dynnikov., Semiclassical motion of the electron. A proof of the Novikov conjecture in general position and counterexamples., Solitons, geometry, and topology: on the crossroad, Amer. Math. Soc. Transl. Ser. 2, 179, Amer. Math. Soc., Providence, RI, 1997, 45-73.
- [10] I.A. Dynnikov., The geometry of stability regions in Novikov's problem on the semiclassical motion of an electron., *Russian Math. Surveys* **54**:1 (1999), 21-59.
- [11] I.A. Dynnikov., Interval Identification Systems and Plane Sections of 3-Periodic Surfaces., *Proc. Steklov Inst. Math.* **263** (2008), 65-77.
- [12] I. Dynnikov, A. Skripchenko., On typical leaves of a measured foliated 2-complex of thin type., Topology, Geometry, Integrable Systems, and Mathematical Physics: Novikov's Seminar 2012-2014, Advances in the Mathematical Sciences., Amer. Math. Soc. Transl. Ser. 2, 234, eds. V.M. Buchstaber, B.A. Dubrovin, I.M. Krichever, Amer. Math. Soc., Providence, RI, 2014, 173-200, arXiv: 1309.4884
- [13] R.N. Gurzhy, A.I. Kopeliovich., Low-temperature electric conductivity of pure metals., In the book: Conductivity electrons., Red. M.I. Kaganov, V.S. Edelman., Moscow, Nauka, 1985 (in Russian).
- [14] A.Ya. Hinchin, Continued fractions., Moscow: FISMAT-GIS, (1961).
- [15] M.I. Kaganov, V.G. Peschansky., Galvano-magnetic phenomena today and forty years ago., *Physics Reports* **372** (2002), 445-487.
- [16] C. Kittel., Quantum Theory of Solids., Wiley, 1963.
- [17] I.M. Lifshitz, M.Ya. Azbel, M.I. Kaganov. *Sov. Phys. JETP* **4** (1957), 41.
- [18] I.M. Lifshitz, V.G. Peschansky., Galvanomagnetic characteristics of metals with open Fermi surfaces., *Sov. Phys. JETP* **8** (1959), 875.
- [19] I.M. Lifshitz, V.G. Peschansky., Galvanomagnetic characteristics of metals with open Fermi surfaces. II., *Sov. Phys. JETP* **11** (1960), 137.
- [20] I.M. Lifshitz, M.I. Kaganov., Some problems of the electron theory of metals I. Classical and quantum mechanics of electrons in metals., *Sov. Phys. Usp.* **2**:6 (1960), 831-835.
- [21] I.M. Lifshitz, M.I. Kaganov., Some problems of the electron theory of metals II. Statistical mechanics and thermodynamics of electrons in metals., *Sov. Phys. Usp.* **5**:6 (1963), 878-907.
- [22] I.M. Lifshitz, M.I. Kaganov., Some problems of the electron theory of metals III. Kinetic properties of electrons in metals., *Sov. Phys. Usp.* **8**:6 (1966), 805-851.
- [23] I.M. Lifshitz, M.Ya. Azbel, M.I. Kaganov., Electron Theory of Metals. Moscow, Nauka, 1971. Translated: New York: Consultants Bureau, 1973.
- [24] A.Y. Maltsev., Anomalous behavior of the electrical conductivity tensor in strong magnetic fields., *JETP* **85** (5) (1997), 934-942.
- [25] A.Ya. Maltsev, S.P. Novikov., Quasiperiodic functions and Dynamical Systems in Quantum Solid State Physics., *Bulletin of Braz. Math. Society, New Series* **34**:1 (2003), 171-210.
- [26] A.Ya. Maltsev, S.P. Novikov., Dynamical Systems, Topology and Conductivity in Normal Metals in strong magnetic fields., *Journal of Statistical Physics* **115**:(1-2) (2004), 31-46.
- [27] S.P. Novikov., The Hamiltonian formalism and a many-valued analogue of Morse theory., *Russian Math. Surveys* **37** (5) (1982), 1-56.
- [28] S.P. Novikov, A.Y. Maltsev., Topological quantum characteristics observed in the investigation of the conductivity in normal metals., *JETP Letters* **63** (10) (1996), 855-860.
- [29] S.P. Novikov, A.Y. Maltsev., Topological phenomena in normal metals., *Physics-Uspekhi* **41**:3 (1998), 231-239.
- [30] T. Osada, S. Kagoshima, N. Miura., Resonance effect in magnetotransport anisotropy of quasi-one-dimensional conductors., *Phys. Rev. B* **46**:3 (1992-I), 1812.
- [31] Ya.G. Sinai, K.M. Khanin., Mixing for some classes of special flows over rotations of the circle., *Functional Analysis and Its Appl.* **26**:3 (1992), 155-169.
- [32] A. Skripchenko., Symmetric interval identification systems of order three., *Discrete Contin. Dyn. Sys.* **32**:2 (2012), 643-656.
- [33] A. Skripchenko., On connectedness of chaotic sections of some 3-periodic surfaces., *Ann. Glob. Anal. Geom.* **43** (2013), 253-271.
- [34] S.P. Tsarev. Private communication. (1992-93).
- [35] J.M. Ziman., Principles of the Theory of Solids., Cambridge Univ. Press 1972.
- [36] A.V. Zorich., *Russian Math. Surveys* **39**, 287 (1984).
- [37] A.V. Zorich., Proc. "Geometric Study of Foliations".,

(Tokyo, November 1993) / ed. T.Mizutani et al. Singapore: World Scientific, 479-498 (1994).

- [38] We do not consider here the spin variables, which will not play an essential role in our picture.
- [39] We would like to emphasize here that for generic Fermi level  $\epsilon_F$  the measure of the stable open trajectories on the Fermi surface remains finite up to the boundary of the “mathematical Stability Zone”  $\Omega_\alpha$ . However, it is often assumed in the literature that this measure vanishes at the boundary of a Stability Zone on the angle diagram, which seems to be in accordance with experimental data. As we will see below, the last circumstance is caused by the existence of an extended “experimentally observable” Stability Zone  $\hat{\Omega}_\alpha$  including an additional region  $\Lambda_\alpha$ , adjacent to the boundary of  $\Omega_\alpha$ , with very special behavior of trajectories of system (I.1). It will be also shown, that the presence of additional Zone  $\Lambda_\alpha$  is responsible also for arising of rather nontrivial analytical regimes of conductivity behavior in the extended Zone  $\hat{\Omega}_\alpha$ .
- [40] Let us say here that the presence of additional segments adjacent to the Stability Zone on the angle diagram and corresponding to the presence of periodic open trajectories on the Fermi surface was discussed in the literature (see e.g. [15, 18–23]). It is often assumed, however, that

this set is given by a finite number of segments, corresponding to some special (main) rational directions  $\mathbf{a}$ . As we could find, the first indication of the existence of an everywhere dense set of additional directions of  $\mathbf{B}$  near the boundary of the zone of stable open trajectories, corresponding to the appearance of periodic trajectories of the system (I.1), was given in the work [13]. Let us say here, that the example in the work [13] is connected with the system (I.1) on a special Fermi surface of genus 2, which are not considered as complex according to our terminology. However, an analogous property is also true in the general case for the Stability Zones on arbitrarily complex Fermi surfaces. This fact is connected actually with a special structure of the system (I.1) (and the existence of topological quantum numbers) at  $\mathbf{B}/B \in \Omega_\alpha$ , which is a consequence of rather nontrivial topological theorems ([8, 36]) in the general case. We would like to emphasize here that the additional segments arise for every curve  $\gamma_{\mathbf{a}}^\alpha \subset \Omega_\alpha$  connected with a rational mean direction of open trajectories of (I.1). As a result, these segments form a dense set near the boundary of  $\Omega_\alpha$ , which plays an important role in the formation of additional “experimentally observable” Zone  $\Lambda_\alpha$  around the exact mathematical Stability Zone  $\Omega_\alpha$ .